

## ELECTROCHEMICAL ANALYSIS OF SOLIDS. A REVIEW

Tomáš GRYGAR<sup>a,\*</sup>, Frank MARKEN<sup>b</sup>, Uwe SCHRÖDER<sup>c1</sup> and Fritz SCHOLZ<sup>c2</sup><sup>a</sup> Institute of Inorganic Chemistry, 250 68 Řež, Czech Republic; e-mail: grygar@iic.cas.cz<sup>b</sup> Department of Chemistry, Loughborough University, Epinal Way, Loughborough, Leicestershire, LE11 3TU, U.K.; e-mail: f.marken@lboro.ac.uk<sup>c</sup> Institute of Chemistry, E.-M. Arndt University Greifswald, D-17489 Greifswald, Germany; e-mail: <sup>1</sup> uweschr@uni-greifswald.de, <sup>2</sup> fscholz@uni-greifswald.de

Received November 21, 2001

Accepted December 30, 2001

1. Introduction . . . . .	164
2. Basics and Milestones . . . . .	165
3. Techniques for Electrode Preparation. . . . .	167
3.1. Compact Crystal Electrodes . . . . .	167
3.2. Composite Electrodes . . . . .	168
3.3. Film Electrodes with Embedded Particles . . . . .	171
3.4. Direct Immobilisation of Solid Particles . . . . .	172
3.5. Comparison of the Techniques . . . . .	173
4. Electrochemical Techniques for Solid-State Systems . . . . .	174
4.1. Voltammetric and Chronoamperometric Measurements . . . . .	174
4.2. Hyphenated Techniques . . . . .	175
5. Solid-State Electrochemical Analysis and Characterisation . . . . .	177
5.1. Which Electrochemical Characteristics are Evaluated? . . . . .	179
5.2. Reproducibility and Detection Limits . . . . .	183
5.3. Examples of Electroanalysis of Inorganic Solids . . . . .	184
5.3.1. Elemental and Phase Analysis . . . . .	184
5.3.2. Solid Solutions . . . . .	186
5.3.3. Stoichiometry of Metal Oxides and Chalcogenides . . . . .	192
5.3.4. Identification/Characterisation of Redox Centres in Solids, Redox-Based Speciation in Solid State . . . . .	193
5.3.5. Particle Size and Crystallinity . . . . .	194
5.4. Examples of Electroanalysis of Organic and Organometallic Solids . . . . .	196
6. Future Prospects . . . . .	202
7. References . . . . .	203

The topic of the review is the electrochemical analysis of solids aimed to identify or determine their phase or elemental composition, analyse the composition of solid mixtures, characterise their electrochemistry-related properties and analyse the redox state of the constituent elements. The ways of the electrode preparation are discussed with a special attention paid to compact and composite electrodes including carbon-paste electrodes, and di-

rect immobilisation of powders on a working electrode. Examples are given of simultaneous electrochemical measurements combined with X-ray diffraction, optical or atomic force microscopy, and mass measurement by quartz microbalance. The state-of-art of voltammetric analysis of inorganic and organic solids achieved in the last two decades is systematically reviewed with the aim to find cases, when electrochemistry can compete successfully with other analytical techniques as for sensitivity, specificity, and sample consumption. Electrochemical methods are shown to be a perspective tool for redox analysis of catalysts, combined elemental and phase analysis of inorganic pigments and minerals, characterisation of solid solutions, metalloorganic and organic solids. A review with 196 references.

**Keywords:** Solid-state chemistry; Powders; Analytical methods; Voltammetry; Electrochemistry.

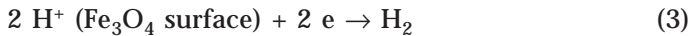
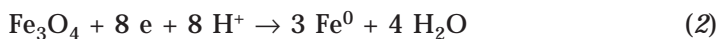
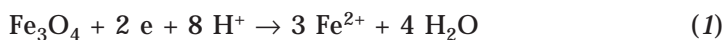
## 1. INTRODUCTION

Solid phases are traditionally characterised by elemental analysis, diffraction, spectroscopic, microscopic, and separation techniques. A complementary and very versatile tool for solid-state characterisation may be based on electrochemistry<sup>1,2</sup>. Solid-state electrochemical techniques have been important for the study of intercalation processes and for battery materials, but may also be applied to a much wider range of solid materials. Electrochemical characteristics, such as the formal potentials for solid-state redox pairs as a function of the solution environment and the ability of the solid to undergo reversible ion insertion processes, are important and not always fully explored or understood. Furthermore, electrochemistry can provide additional analytical information, allowing the identification of structural features or distinct solid phases, the homogeneity of the sample or the presence of different solid species, and in some cases the quantitative analysis and composition of the solid.

The term electrochemical analysis has been used for divergent techniques ranging from traditional polarography of soluble metal ions to the characterisation and optimisation of solid fuel-cell components. This review focuses on the analysis of powders and other forms of solids by electrochemical techniques, leading to qualitative and quantitative compositional information and to characterisation of chemical and electrochemical solid-state properties. Electrochemistry yields specific information on the kinetics and thermodynamics of the reactions of solids that can be related to their structure and composition. However, for the detailed interpretation of results from solid-state electrochemical experiments, complementary data obtained by traditional methods or structural information obtained by comparison and analogy with reference materials are required.

## 2. BASICS AND MILESTONES

Metals were among the first solids systematically investigated in electrochemistry, especially with respect to their corrosion properties. The aim was predominantly practical: to identify conditions suitable for metal passivation or, oppositely, to investigate which potentials and ions enhance corrosion. Metal alloys were first analysed using electrography<sup>3</sup>. Corrosion products, such as metal oxides and hydroxides formed at the surface of these metals, were subsequently studied. However, secondary solid phases formed *in situ* are not always crystalline and well defined and a need arose for the study of independently synthesised metal compounds. Important steps towards the electroanalysis of solids were taken in pioneering work with compact electrodes of conducting compounds, such as  $\text{Fe}_3\text{O}_4$  (refs<sup>4–6</sup>), which is an important component of oxide layers on iron and steel surfaces, and nuclear fuel  $\text{UO}_2$  (refs<sup>7,8</sup>). These studies have revealed the multi-step and potential-dependent nature of the electrochemical dissolution process, consisting of surface conditioning in the aqueous phase, redox change at the solid surface, and diffusion of soluble products. The colourful electrochemistry of  $\text{Fe}_3\text{O}_4$  may serve as an example: the interfacial redox chemistry may involve reductive dissolution (Eq. (1)), reduction to metallic iron (Eq. (2)), or catalytic hydrogen evolution (Eq. (3)). These processes yield one separated and one multicomponent voltammetric peak.



Battery and energy-storage system research was a further major source of knowledge on electrochemical solid-state reactivity. In particular  $\text{MnO}_2$  was studied extensively in the early 1970's, but mainly with focus on practical aspects, such as the specific charge capacity, the rechargability, and the stability in the time and the number of charge/discharge cycles. Many mechanistic aspects of the complex solid-state electrochemical process hence remain unresolved. Similarly, in corrosion science, a huge literature on practical electrochemical characteristics has been accumulated. In spite of the progress in equipment, measuring techniques, and theory, the direct

impact of solid-state electroanalysis on a wider range of chemical problems was of low significance.

The introduction of carbon paste electrodes (CPE) was an important step toward practical solid-state electroanalysis. Traditionally, CPEs are composed of carbon with an organic binder (such as Nujol or silicone oil) and they have been used as analytical electrodes instead of mercury or solid electrodes<sup>9</sup>. If the solid to be studied is added into the paste, the electrode is called “modified CPE” or “carbon paste electroactive electrode” (CPEE). The CPEE was introduced by Kuwana and French<sup>10</sup> to obtain potentials of redox reactions of *sparingly soluble* organic compounds, which would have otherwise required utilisation of polarography in organic solvents with a much bigger sample consumption. The CPEE methodology was soon recognised to be also suitable for *insoluble* electroactive compounds (AgBr (ref.<sup>11</sup>), CuS, PbS, and ZnS (ref.<sup>12</sup>)). It has been observed that for these insoluble materials no dissolution prior to electrochemical reactions is required. The first studies of metals, metal oxides, chalcogenides, salts and other compounds by CPEE methodology were reviewed by Brainina *et al.*<sup>1,13</sup> and Kalcher *et al.*<sup>14</sup>. Lecuire<sup>15</sup> investigated the reaction stoichiometry of Fe oxides in CPEEs and demonstrated the determination of the mass of the solid reactant by measuring the charge consumed in the course of the electrochemical process. This analysis was possible without the need of a calibration plot because it was strictly based on the Faraday law. The CPEE methodology significantly increased the scope of electrochemistry to poorly conducting and insoluble solids and enabled the first analytical applications of solid-state electrochemistry. CPEEs are currently mainly used for studying interactions of solids with dissolved species. Some solids employed for modifying CPEs, *e.g.* clays<sup>16</sup> and zeolites<sup>17</sup>, significantly improve their specificity or sensitivity in the quantitative analysis of a dissolved target species<sup>14</sup>.

The voltammetry of microparticles (VMP, formerly abrasive stripping voltammetry) methodology based on the mechanical immobilisation of solid particles at the surface of carbon or metal electrodes in the absence of binders (Scholz *et al.*<sup>18,19</sup>), broadened the possibilities of solid-state electroanalysis due to its broad applicability. The VMP method is attractive also due to the ease of preparation of the solid sample and the short time scale required for an electrochemical measurement (see recent review by Scholz and Meyer<sup>2</sup>). The technique allows real-time monitoring of reactions by *in situ* spectro-electrochemical methods<sup>2</sup>. VMP has become an important step towards direct analysis of well-defined solid powders without their further pretreatments or time-consuming deposition procedures.

The electrochemical analysis of solids was proposed as an alternative approach to traditional analytical and characterisation techniques, for example in reviews on CPEE methods by Brainina and Vydrevich<sup>13</sup>, on advanced materials by Rusling and Suib<sup>20</sup>, and on VMP by Scholz and Meyer<sup>2,21</sup>. This review focuses on methods and important developments in solid-state electrochemistry. Detailed studies of battery materials are beyond the scope of this review, unless they have a more general impact on characterisation methods of solids. Also omitted are all-solid electrochemical cells without a liquid phase (solution of supporting electrolyte), which are used for the analysis of materials for solid electrochemical devices<sup>22</sup> and for gas-solid cells of gas sensors<sup>23</sup>.

Although of considerable importance to the study of solid-state electrochemical processes, and in particular for surface redox reactions, recent developments in *in situ* surface characterisation by scanning probe methodologies<sup>24</sup> will be mentioned only briefly where relevant to analytical applications. In future, these high spatial resolution techniques (which currently still require single crystal surfaces or very well defined crystalline surface sites) and scanning electrochemical microscopy methods will help improve the knowledge on solid-state electrochemical processes.

### 3. TECHNIQUES FOR ELECTRODE PREPARATION

The method of preparation of a solid sample for electrochemical measurement is not a standard task such as, for example, the filling of the sample holder for X-ray powder diffraction. For the electrochemical measurement the sample particles must have sufficiently good electric contact with the electrode (current collector) and also with the solution phase supplying ions. For practical analytical purposes, the technique should be simple, reliable, and either universal or at least suitable for a well-defined range of applications.

#### 3.1. Compact Crystal Electrodes

The compact electrode (CE) is a compact body, such as pellet, disk, or rod made of the material to be studied, used as the working electrode. CEs are only suitable for good electric conductors, such as metals,  $\text{Fe}_3\text{O}_4$  (refs<sup>4–6,25,26</sup>) or  $\text{UO}_2$  (refs<sup>7,8</sup>). This technique was also used for chalcogenides such as  $\text{Cu}_x\text{S}$  (refs<sup>27,28</sup>),  $\text{PbS}$  (ref.<sup>29</sup>), and  $\text{FeAsS}$  (ref.<sup>30</sup>). The need to study poorly electrically conducting materials revealed the limit of compact electrodes: The ohmic resistance of the solid between the active surface and

current collector causes distortion of voltammetric curves according to the Ohm law (so-called *iR* drop). In studies of the electrochemical behaviour of  $\text{FeS}_2$ , the problem of low conductivity was attempted to be solved by using a “slurry electrode” (suspension of solid particles with an inert electric contact immersed in the suspension<sup>31</sup>). Another approach was to immobilise pyrite particles in a polymer film on an electrode<sup>32</sup> (more details are given in Part 3.3.).

Studies on organic CEs have also been conducted but the low electrical conductivity of most organic materials prevents more wide-spread application. Very thin single-crystalline films of anthracene derivatives have been studied for photoelectrochemical processes<sup>33,34</sup> and direct electrochemistry at CEs made of electrically conducting charge-transfer salts, *e.g.*  $\text{TTF}^+[\text{TCNQ}^-]$  (TTF, tetrathiafulvalene; TCNQ, 7,7,8,8-tetracyanoquinodimethane) has been investigated<sup>35</sup>. In other studies employing very thin films of organic or organometallic materials, *e.g.* phthalocyanine metal complexes<sup>36</sup>, pores in the thin film deposit are involved in the overall process and therefore these systems may not be regarded as real CEs.

Analytical applications of CEs are rather exceptional because their preparation is usually laborious and requires special procedures, such as pressing and sintering. Under high pressure and temperature, the stoichiometry and phase composition of the powders to be analysed could be changed. The CE technique is currently mainly used to study surface electrochemistry of naturally occurring minerals and their interaction with solutions. For example, galena ( $\text{PbS}$ ) electrochemistry was studied in relation to its flotation<sup>29</sup>, and magnetite,  $\text{Fe}_3\text{O}_4$  and ilmenite,  $\text{FeTiO}_3$  to their weathering<sup>26</sup>. The electrochemistry of single surfaces of monocrystals, including their adsorption properties, has been reviewed elsewhere<sup>24</sup> and will not be covered here. This technique is not used routinely but rather for sorption studies and fundamental electrochemistry.

### 3.2. Composite Electrodes

Composite electrodes contain the solid to be studied mixed with a conductive additive (usually carbon black, “acetylene black” or milled graphite) and possibly a binder to improve mechanical properties of the composite. The mixture is pressed into a suitable holder (cup), or spread over or pressed to a current collector, such as a metal mesh or plate. Mixtures for battery electrodes are of a similar nature. This concerns both laboratory research and practical electrochemical cells. Battery development also fuelled the search for the carbon particles with the best redox stability and for

polymeric binders with the best mechanical properties. Recently the development of  $\text{Li}^+$  ion batteries has promoted very systematic interest in composite electrodes, which should possess an extreme long-term stability in the order of thousands of discharge–recharge cycles. Also electrodes designed for fuel cells operating under ambient temperatures in liquid or membrane electrolyte are based on mixtures of a catalyst, carbon and binder that should have extremely high durability, and low resistance to electron and mass transport. Teflon suspensions and poly(vinylidene difluoride) are the most popular binders in those energy devices.

In electrochemical analysis of solids, composite electrodes are usually denoted as carbon paste electrodes or carbon paste electroactive electrodes, and organic oil (e.g., silicone oil) or electrolyte (e.g., aqueous acid) are used as a binder. CPEEs are related to paste electrodes popular in electroanalytical chemistry of dissolved species<sup>14,37</sup>. CPEE is a very universal electrode, although its optimisation for quantitative analysis is not a trivial task<sup>38</sup>. Surprisingly, small attention was paid to the properties of CPEE with organic binders, where the hydrophobisation of the solid could possibly alter the resulting electrode kinetics.

CPEEs with non-conducting binders were invented and carefully studied in the former Soviet Union (for a review, see Brainina *et al.*<sup>1,13</sup>). Brainina *et al.* tested them mainly for elemental and phase analyses as an alternative to other instrumental analytical techniques. CPEE remains one of the most flexible electrodes for the study of electroactive solids and interactions of solids with soluble species, including clay-modified electrodes, sensors, *etc.* However, the hydrophobic non-conducting binder does not behave as an indifferent component of the electrode but affects the results in a certain manner. In CPEE, the reaction depth, *i.e.* the fraction of the paste involved in the electrochemical reactions, depends on the kind of binder (silicone oil differs from dibutyl phthalate), probably due to different binder hydrophobicity<sup>38</sup>. Similarly to the case of CPE and dissolved ferri-/ferrocyanide analyte<sup>39</sup>, also in CPEE with solid TiC analyte<sup>38</sup>, the peak current decreases with increasing amount of organic binder in the carbon paste. On the other hand, Zakharchuk *et al.*<sup>40</sup> did not observe any adverse influence of silicone oil binder on the behaviour of Pb oxides in CPEE. It is hence recommendable to evaluate the binder effect on each individual solid to be analysed.

When organic binders are used, organic materials usually dissolve in the binder. Therefore, the possibilities of studies of solid-state properties of these materials are very limited, even though more complex biological materials such as enzymes<sup>41</sup> and whole cells<sup>42</sup> have been successfully immobilised and investigated. A study, in which both voltammetry and bulk

electrosynthesis of insoluble organic compounds were realised by mixing graphite and organic solid without binder, was reported<sup>43</sup>.

CPEE with an aqueous electrolyte solution as binder is suitable for both soluble and insoluble species and hence also makes it possible to compare and dissect distinct electrochemical processes. The binder is usually a dilute mineral acid that commonly partly dissolves the solid to be studied already before the electrochemical measurement<sup>44</sup> and accumulates all soluble and solid reaction products. As a result of a limited volume of the electrode system, voltammograms of a complex shape are obtained with such electrodes. A simple procedure to distinguish the contribution from solid and soluble electroactive species was proposed by Encinas Bachiller *et al.*<sup>45</sup>, who let the solid to be studied equilibrate with the binder, and used the filtrate as a binder in plain CPE without adding the solid to the paste. Such experiments help understand the voltammogram obtained with a paste containing the solid by identifying the voltammetric peaks caused by the dissolved species. A more recent technique for the study of solids has been proposed, based on screen printing of a modified paste<sup>46</sup>. This technique is highly reproducible, although more laborious than the conventional making of paste electrodes.

Although the amount of analyte in the CPEE with an electrolytic binder is known, this does not necessarily mean that all the analyte introduced in the paste electrode is involved in the reaction. The charge efficiency of CPEE depends on the actual electrode composition, the amount and kind of the solid analyte, and on the electrode construction. For example, for Fe oxides in CPEE with an aqueous acid as binder, Lecuire<sup>15</sup> and Mouhandess *et al.*<sup>44</sup> reported a complete conversion of Fe oxides, but the charge efficiency decreased to few tens of per cent or less for  $\text{Fe}_2\text{O}_3$  with large, sintered particles and for some ferrites<sup>44</sup>. Passivation can also decrease the reaction yield<sup>38</sup>. Another reason for the decrease can be a too large load of the electroactive solid in the electrode, as was shown for ferrocene by Bauer and Gaillochet<sup>47</sup> and lately by Ramírez *et al.*<sup>48</sup>. A few per cent of electroactive species in the paste is a recommendable load.

In CPEEs with organic binders, the amount of electroactive solid material is generally not known because only the outermost surface layer of the paste is accessible for ion transfer to or from the electrolyte solution, and it is not known how much of the electroactive solid particles in this layer are covered with protecting layer of the organic binder. In some cases it may also happen that some particles below the surface undergo an electrochemical reaction due to roughening of the surface or dissolution of the outer-

most layer. This uncertainty leads to the necessity of using calibration plots for quantitative analysis.

### 3.3. Film Electrodes with Embedded Particles

A powder sample can be immobilised on an electrode surface by evaporation of its dispersion in an appropriate solvent with an addition of a polymer “glue”. This technique became particularly popular in studies of clay-modified electrodes (first such denotation was used by Ghosh and Bard<sup>49</sup>, the topic was reviewed by Fitch *et al.*<sup>16</sup>). In the 1980's films obtained from suspensions of the solid to be studied, carbon and a polymer (polyvinyl alcohol, polystyrene) were tested for preparation of clay- and zeolite-modified electrodes. The reported conclusions can be summarised in the following points:

- (i) the polymer additive is not necessary for the electrode preparation<sup>50</sup>;
- (ii) reproducibility and stability of the carbon-zeolite-silicone oil composite electrode are better than those of zeolite-polystyrene coated electrode<sup>51</sup>;
- (iii) in the absence of carbon, only the layer of particles adjacent to the electrode support is active<sup>52,53</sup>.

In analytical applications, limited durability and poor reproducibility of polymer-film composite electrodes were often observed, probably partly due to the low conductivity of the zeolites and clay components.

For organic redox-active solid thin films of Nafion<sup>TM</sup>, cation exchange membrane has been employed to stabilise electrochemical responses. The solid-to-solid conversion of tetrathiofulvalene in a Nafion<sup>TM</sup> film has been characterised by Bard and co-workers<sup>54</sup>. The solid-to-solid redox process occurring in reduction of tetracyanoquinodimethane (TCNQ) has been studied extensively; by applying a very thin coating with Nafion<sup>TM</sup>, electrochemical responses were “stabilised”<sup>55</sup>.

Polymer film electrodes have recently been successfully used by Doménech-Carbó *et al.*<sup>56–59</sup>, who preferred this technique to be able to work with samples of fine arts, such as pigments of paintings and sculptures and weathering crusts on glass. Actually, the limited sample amount available dictated to use this kind of electrode. Doménech-Carbó *et al.* evaporated a known amount of suspension of 0.1 mg sample in acetone solution of poly(methyl methacrylate) on a carbon electrode. The resulting film contains pores that permit the exchange of ions between solution and electrode surface. Optimum film electrodes were obtained with final coverage by polymeric component and sample at the surface load of 0.8 and

0.2–0.4 mg cm<sup>-2</sup>, respectively<sup>57</sup>. The electrode was suitable for analyses by single-scan direct or stripping voltammetry<sup>57,60</sup>.

### 3.4. Direct Immobilisation of Solid Particles

Solids and in particular powders can be directly deposited on suitable electrode surfaces without the necessity of mechanical pretreatment or the presence of additives, such as binders required in composite electrodes. In 1982 Roullier and Laviron<sup>61</sup> explored the electrochemical properties of some organic solids (phenazine, azobenzene, chloranil) deposited as a “thick layer” onto electrodes by evaporation of a solution of these compounds in a volatile solvent. The electrode was immersed in an aqueous solution. It was proposed that although a direct solid-to-solid reaction was possible, a dissolved intermediate was likely to participate in the overall solid redox process in these systems.

Although allowing insights into solid-state redox processes, experiments based on thick-film deposits suffer drawbacks from high currents and resistance effects. In contrast, the voltammetry of microparticles procedure is based on a mechanical (abrasive) deposition of traces (submilligram amounts) of samples on a sufficiently soft working electrode, usually pyrolytic graphite, paraffin-impregnated graphite, pencil lead<sup>62</sup>, or gold in *in situ* quartz crystal microbalance techniques. The method is the least laborious technique for preparation of a solid for electrochemical measurements and is suitable for relatively soft compact samples (metals) and any powder. Polycrystalline boron-doped diamond has recently been suggested as an electrode material suitable for immobilisation of harder microparticles including iron and brass<sup>63</sup>. Most studies have been carried out at macroelectrodes of typically 5 mm diameter. However, single particles have been attached to a microelectrode with a micromanipulator<sup>64</sup> to remove the influence of ill-defined sample geometry in the composite electrode. In macroscopic electrodes, a drawback of the VMP method is that the amount of the material deposited is difficult to control. On the other hand, the VMP procedure is very flexible in allowing a huge range of solids to be studied and compared voltammetrically irrespective of their synthesis, origin, or pretreatment. This includes a wide range of organic or molecular materials that are relevant as novel energy storage materials, important in industrial redox dissolution, or in electrochemical synthesis.

Aggregates of particles can be easily physically attached to a current collector by evaporating the slurry (suspension) of solid onto an appropriate current collector. This slurry deposition has been used in a study of electro-

catalytic properties of powdered compounds<sup>65</sup> and also for an *in situ* atomic force microscopy electrochemical study of PbO reduction<sup>66</sup>. Similarly, electrodes for quartz-microbalance measurements can also be prepared by slurry evaporation and heat treatment. Assemblage of solid particles physically adhered to the current collector, can also be prepared by brushing<sup>67</sup> or spraying<sup>68</sup> solutions of soluble precursors and subsequent drying and calcination to obtain a layer of the solid to be studied on the electrode surface. Simple pressing of powders onto metal-mesh current collectors was used to study a CuO-ZnO catalyst<sup>69</sup>.

### 3.5. Comparison of the Techniques

In Parts 3.1 to 3.4 it has been shown that each kind of electrode has its own limitations and can affect the results of the electrochemical measurement. The comparison of more techniques of the electrode preparation should unequivocally exclude that the technique affects the characteristics, which will exclusively be attributed to the analyte. Ferrocene/ferrocenium electrochemistry, studied in CPEEs with conducting binders, is an example of an electrode systems, whose preparation significantly affects the voltammetric peak potential: 150 mV difference was found by Ramírez *et al.* just due to a different electrode preparation<sup>48</sup>. The reason for different results obtained with CPEEs with ferrocene probably arose due to the different kinetic regimes (thin-layer behaviour, bulk diffusion in the paste, and electrochemically promoted dissolution). The kinetic regimes were evaluated according to the shape of the chronoamperometric curves<sup>48,70,71</sup>.

A systematic comparison of VMP and CPEE was undertaken with cyano-metallates that yield reversible ion insertion/extraction when in contact with aqueous electrolyte solutions. VMP and voltammetry with thin films of Prussian blue (iron hexacyanoferrate) were compared by Dostál *et al.*<sup>72</sup>. No systematic influence of the technique of electrode preparation on electrochemical behaviour was found with respect to the electrochemical potentials and the reaction course. CPEEs with non-conducting binder and VMP were compared by Zakharchuk *et al.*<sup>73</sup>, who found that the electrochemistry of Prussian blue was very similar for both types of electrodes and the hydrophobic binder of CPEE only slightly affected the observed reversibility of redox reactions. More significant differences were shown in another report by Zakharchuk *et al.*<sup>40</sup>, who used VMP and CPEE with non-conducting binder in the case of yellow and red PbO,  $\alpha$ - and  $\beta$ -PbO<sub>2</sub>, and BaPbO<sub>3</sub>. The study showed qualitative and quantitative differences between the two electrodes, regarding voltammetric peak potentials and peak

shapes. In acid solutions the behaviour of lead oxides in CPEE with non-conducting binder was surprisingly more reversible, voltammetric peaks were narrower and, hence, peak separation of overlapping processes was better than using VMP. In alkaline solution, the differences were less dramatic.

The solids, that were also studied using several techniques of electrode preparation, are battery materials.  $\text{Li}_x\text{Mn}_2\text{O}_4$  and  $\gamma\text{-MnO}_2$  were characterised with VMP and composite electrode<sup>74,75</sup>,  $\text{MnO}_x/\text{C}$  with VMP, CPEE with conducting binder, and Teflon-bonded composite electrode<sup>76</sup> and  $\text{LiCoO}_2$  battery materials with single-particle electrode and composite electrode<sup>64</sup>. It is not surprising that due to the sluggishness of the mass transport through the solids or the mass of the electrode composite, the electrodes with finely dispersed particles such as those with VMP or single-particle electrode permit to use a faster scan rate, getting better resolved voltammograms than upon using much thicker composite electrodes. On the other hand, composites with a known weight and concentration of solid to be studied are to be used in analyses that should yield specific charges (per amount of reacting substances).

#### 4. ELECTROCHEMICAL TECHNIQUES FOR SOLID-STATE SYSTEMS

##### 4.1. Voltammetric and Chronoamperometric Measurements

Most studies on solid-state redox systems are at least initially based on cyclic voltammetry. In cyclic voltammetry, the potential of the working electrode is scanned linearly between two threshold values and the current is recorded. A wealth of information about the potential region where redox processes occur, the reversibility and type of processes, and the nature of reaction products are obtained. By varying the scan rate applied in the course of the experiment, the time scale of processes can be explored. It is recommended for all types of solid-state redox systems to establish first the open-circuit (or zero-current) potential. This equilibrium potential is important as the starting potential for linear-potential scan studies. Without the knowledge of the open-circuit potential, important information may be lost during the switching-on process before data collection<sup>77</sup>.

With the knowledge from cyclic voltammetric experiments, it is possible to employ more detailed chronoamperometric or impedance techniques. Only recently, a novel and very useful electrochemical method based on *in situ* resistometry<sup>78</sup> has been proposed.

Although electrochemical procedures allow a considerable insight into the redox processes that occur at the triple interface solid particle|electrode|solution (electrolyte), the complexity of this kind of system requires the use of additional or complementary tools. In the next section, the options of coupling of electrochemical with spectroscopic or other methodologies in hyphenated techniques are summarised.

#### 4.2. *Hyphenated Techniques*

The depth of information about the course of an electrochemical reaction accessible by electrochemical techniques is always limited. This particularly applies to reactions that involve more than one charge transfer step and also to reactions of solids that are very much dependent on parameters like morphology, crystallinity, and defect structure of the studied compounds. Hyphenated techniques, *i.e.* *in situ* combinations of electroanalytical techniques with other analytical techniques have proved to be highly powerful tools to gather information about electrode processes that for electroanalytical techniques alone would not be accessible. For the study of solid-state electrochemical reactions, a number of *in situ* combinations have been developed, including *in situ* spectroscopic (“spectroelectrochemical”) techniques, the electrochemical quartz crystal microbalance as well as the surface probing techniques like the atomic force microscopy.

One of the widest spread and most versatile hyphenated techniques for the study of solid compounds is the electrochemical quartz crystal microbalance (EQCM). The technique allows to continuously monitor mass changes at an electrode surface with a sensitivity of few nanograms by means of tracking the resonance frequency of the resonator, a gold-coated quartz crystal that serves at the same time as the working electrode in the electrochemical experiment. EQCM measurements have been widely used for the study of dissolution and passivation reactions of metals and alloys under electrochemical and chemical corrosion conditions. Bond *et al.*<sup>79,80</sup> used the electrochemical quartz crystal microbalance to analyse electrochemically and chemically induced dissolution reactions of C<sub>60</sub> fullerenes. Another domain of EQCM is the examination of (topotactic) solid-solid reactions (transformations)<sup>81</sup>. Here, EQCM helps in identifying the nature of charge-compensating ion transfers between the electrolyte phase and the solid. Examples are the analysis of redox reactions and lattice reconstruction processes of insoluble cyanometallates<sup>72,82</sup>, and the elucidation of the reaction pathways of organic<sup>83</sup> and organometallic<sup>84</sup> solids.

An *in situ* phase identification by means of recording the X-ray powder diffraction patterns during the reduction of mechanically attached microparticles of litharge ( $\alpha$ -PbO) and of laurionite ( $\text{Pb}(\text{OH})\text{Cl}$ ) enabled Meyer *et al.*<sup>85</sup> to discover different reaction schemes for the reductive formation of metallic lead at the surface of a graphite electrode<sup>66</sup>. The authors showed that at room temperature and in the presence of an aqueous electrolyte solution, the reduction of litharge leads to a simultaneous formation of a crystalline lead phase, whereas the formation of lead from laurionite proceeds via an amorphous intermediate, from which a slow crystallisation of lead microparticles takes place.

*In situ* surface microscopic techniques like the atomic force microscopy (AFM) and scanning tunnelling microscopy (STM) usually require sample surfaces to be as smooth as possible and are therefore domains for the study of single crystals and of well defined crystalline surfaces<sup>24</sup>. However, already the first studies utilising AFM for the investigation of microcrystalline compounds illustrated which impact these surface-probing techniques can have in the future on the investigation of solid-state electrochemical reactions. The application of AFM in the study of microcrystalline solids is much more straightforward than that of STM, as it does not require the substrate to be electronically conducting. The main information is the morphology of the electrode surface and of the attached microcrystals. Only recently, Hasse and Scholz<sup>66</sup> presented an *in situ* atomic force microscopic study of the electrochemical reduction of litharge ( $\alpha$ -PbO). The authors attached nanocrystals of the compound at a gold electrode by precipitating it from a suspension of  $\alpha$ -PbO in acetonitrile. With this technique they could confirm the results of Meyer *et al.*<sup>85</sup>, regarding an epitactic solid-state reaction mechanism of the electrochemical lead formation.

Suarez *et al.*<sup>86</sup> studied the reaction pathways of solid 7,7,8,8-tetracyano-quinodimethane mechanically attached to the surface of a glassy carbon electrode. They observed recrystallisation and redistribution of the deposited material during the electrochemical reduction of TCNQ, which supports the assumption of a reaction mechanism involving the electrolyte phase. In a further work, Suarez *et al.*<sup>87</sup> used the *in situ* AFM to monitor morphology changes of  $\text{C}_{60}$  microcrystals. They found very similar results for mechanically attached microparticles as for  $\text{C}_{60}$  deposited by an evaporation technique from a toluene solution.

In many cases the visual observation of the studied sample during voltammetric experiments can deliver valuable information about the state of the solid at the electrode surface. *In situ* light microscopy is a cheap and straightforward technique that enables the reaction to be followed with a

spatial resolution down to a micrometer scale. Compared to AFM, this resolution appears rather low, but considering the cost of the equipment, the possible real-time observation of the electrode surface and additional information like colour changes during the reaction, the *in situ* light microscopy has its advantages. An electrochemical cell that enabled the *in situ* microscopic observation of electrochemical reactions of microcrystalline samples mechanically attached to the surface of paraffin-impregnated graphite electrodes, was presented by Schröder *et al.*<sup>88</sup>. A similar technique was used by Bond *et al.*<sup>55</sup>, who additionally employed a video capturing system for a subsequent analysis of the optical data. Bond *et al.*<sup>89</sup> used the optical microscopy to identify reaction products during the redox cycling of TCNQ by observing the colour change of mechanically immobilised microcrystals and to assess if the reaction can be considered as surface-confined or proceeding through the bulk of the microparticles.

A step ahead compared with this purely visual approach is the *in situ* recording of the microscopic diffuse reflectance of the immobilised microcrystalline samples. This approach helped in unravelling the electrochemical/voltammetric responses of crystalline and amorphous silver octacyanomolybdate and -tungstate, solving questions about the geometric course of their oxidation and reduction. It can also give information on the formation of intermediates and side products during a solid-state electrochemical reaction<sup>90</sup>.

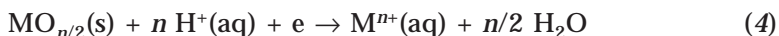
Conventional experimental set-ups for measuring the transmission of optically transparent electrodes can also be utilised. This can be done by mechanically immobilising microparticles at transparent indium tin oxide (ITO) electrodes, as it was done by Bond *et al.*<sup>91</sup> who recorded UV-VIS absorption spectra of indigo during redox cycling and compared the solid-state electrochemistry with the solution electrochemistry of this compound.

## 5. SOLID-STATE ELECTROCHEMICAL ANALYSIS AND CHARACTERISATION

For further discussion, it is necessary to define three basic kinds of reactions of solids at electrodes: (i) electrodissolution, (ii) topotactic solid-to-solid transformation, and (iii) non-topotactic solid-to-solid transformation (see Table I, types A–C). For these reactions, various notations are used and their description requires different phenomenological tools.

Electrodissolution, “stripping” reactions (type A in Table I) are important, for example, in the electroanalysis of dissolved metal ions with chemical or electrochemical preconcentration of solid intermediates at the electrode

surface. Electrodissolution is the conversion of solid species to soluble products, driven by the electrode potential. For the reductive dissolution of metal oxides, for example, the process requires charge neutralisation by protons from the solution phase (Eq. (4)).



Electrodissolution kinetics is discussed in more detail in Part 5.3.5. For its description, heterogeneous reaction kinetics and/or Nernstian diffusion of ions in neighbouring solution are important.

Solid-to-solid transformations can be classified according to the structural relationship between reactant and products. If no recrystallisation is necessary and the host lattice remains intact, as both the reactant and product have very similar structures, the process is “topotactic” according to IUPAC definition (type *B* in Table I). On the other hand if there is a rearrangement of the host lattice during the redox process (or recrystallisation), the pro-

TABLE I  
General evaluation of peak shapes in voltammetry of solids

Type	Requirements for single peaks	Causes of splitting or complex peaks
A Dissolution reactions $\text{s} \rightarrow \text{l}$	Uniform particles of solids Single dissolution mechanism	Bimodal size distribution (see Part 5.3.5) Several kinetic regimes or reaction pathways Highly anisotropic crystals ( $\alpha$ -FeOOH, ref. <sup>104</sup> )
B Reversible ion insertion/extraction reactions (topotactic solid-to-solid transformations)	One kind of redox centres in the solid Single kinetic regime (single diffusion mode) Reagent and products form solid solution	More redox centres (e.g. with different coordination – see Part 5.3.4.) Amorphous fraction in reactants ref. <sup>82</sup> Surface much more reactive than bulk ref. <sup>96,97</sup> Miscibility gap ref. <sup>102</sup>
C Solid-to-solid transformation with recrystallization or substantial re-ordering of crystal structure	Single reaction mechanism and kinetic regime (very rare)	Poor conductivity of intermediates or products ( $\text{MnO}_2$ , ref. <sup>101</sup> ) Recrystallization of thin films of amorphous intermediates on increasing reaction rate

cess is not topotactic (type C in Table I). A redox change in the solid is always accompanied by a movement of ions from/to the solution phase to maintain the charge neutrality. Redox reactions in the solid-state, accompanied by ion expulsion or uptake, are called ion insertion or extraction reactions. Commonly, “intercalation” is used for lamellar systems (layered host structures), but the term is overused also in other ion-insertion reactions.

Topotactic reactions (type B in Table I), such as those of Prussian blue<sup>73</sup>, are chemically reversible and yield stable cyclic voltammograms. Nernst-Peters-like relationships for potential and the Fick diffusion laws are usually used for quantitative data processing. In certain systems, the miscibility gaps in the structure change from reactant to product and must be taken into account to interpret peak splitting and peak separation.

Formally very different are solid systems where the electrochemical conversion is accompanied by a total recrystallization (type C in Table I), because reactants and products are not structurally related and form separate particles. These reactions can be formally divided into chemically reversible (e.g. AgCl/Ag transformation), and chemically irreversible (e.g. Fe<sub>2</sub>O<sub>3</sub>/Fe transformation). However, one must bear in mind that the reversibility is governed by the kinetic regime of the process and therefore depends on the actual reaction rate, the scan rate, temperature, and particle size. In some cases, the kinetics of the solid nucleation must be taken into account to interpret unusual shapes of voltammetric or chronoamperometric curves.

Voltammetry can be also used to characterise electrochemically inactive materials. Such is the case of clay-mineral coated electrode in solution of dissolved electroactive species. The response of such electrode is sensitive to the clay mineral swelling<sup>92</sup>.

### 5.1. Which Electrochemical Characteristics are Evaluated?

Although a huge repertoire of electroanalytical techniques (e.g. pulse techniques, AC impedance, and step techniques) exists, the most attractive approach in solid-state electroanalysis is cyclic voltammetry. In this technique, the potential applied to the working electrode is scanned from an initial value, where no reaction occurs (open circuit potential) to the vertex potential and then, after reversing the scan direction, is scanned back to the initial potential. The peak position ( $E_p$ ), the peak current ( $I_p$ ), and the charge under the peak ( $Q_p$ ) from the resulting current response are important features for analysis. Compared to conventional solution cyclic voltammetry, voltammetric data for solid-state processes are more complex and more difficult to interpret quantitatively. Special care is required when

digital potentiostat systems are employed, as solid systems may give non-conventional current responses and signal distortions due to finite (staircase) step potentials and measuring times may occur (Fig. 1).

**Peak potential ( $E_p$ ).**  $E_p$  is characteristic of the kind of redox species, but is also affected by experimental conditions, in particular scan rate and concentrations of ions involved in the reaction in supporting electrolyte, e.g. protons (Eq. (4)). For a given solid phase, the peak potential depends on a complex of properties sometimes denoted as crystallinity, in particular particle size and uniformity and deviation of stoichiometry. Interpretation of  $E_p$  always requires compounds used as a reference standard, maybe except for reversible systems with tabulated redox potentials, such as some ion-insertion reactions especially in battery materials  $\text{MnO}_2$  and  $\text{Ni}(\text{OH})_2$  or stripping elemental metals by oxidative dissolution. In reversible systems, formal peak potentials are estimated as mean between cathodic and anodic peak potentials,  $E_f = 0.5 (E_{p,a} + E_{p,c})$ , assuming that the diffusion behaves "symmetrically" in the anodic and cathodic directions and the symmetry coefficients are close to 0.5.

If the diffusion processes in adjacent solution limit the reaction rate, the peak potential depends to certain extent on the sample amount on the electrode<sup>40,93</sup> (Fig. 2). In chemically irreversible systems, where reaction kinetics plays a key role, peak potentials are very sensitive to experimental conditions and sample granulometry<sup>13,44,94,95</sup> (Part 5.3.5.).

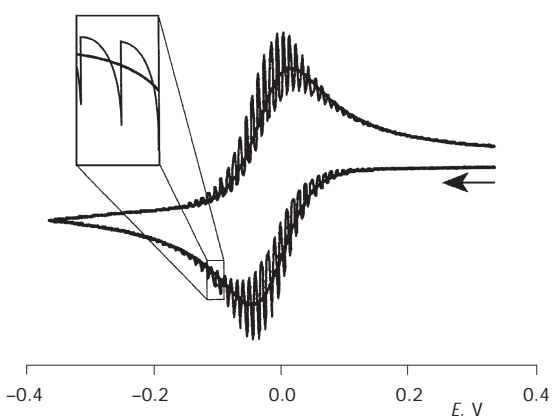


FIG. 1

Distortion of "linear-sweep" voltammetric curve obtained by digital potentiostat with staircase potential programme using too large steps

Mixtures of compounds with different  $E_p$  can be analysed if the  $E_p$  values differ sufficiently. The resolution depends on the peak width; generally, the least resolved difference is 50–100 mV. To improve separation of overlapping redox processes, pulsed techniques can be applied such as differential-pulse and square-wave voltammetry, or more sophisticated techniques used in research of materials for power sources, such as plotting  $\Delta Q/\Delta E$  vs  $E$  (ref.<sup>96</sup>) or step-potential spectroscopy<sup>97</sup>.

*Linear-sweep voltammetric peak shape.* Peak shape is a very sensitive and complex function of several parameters of solid<sup>38,95</sup>, solution, and working electrode<sup>40</sup>. A general overview of voltammetric peak shapes is shown in Table I. For example, bimodal particle size distribution, the presence of more redox sites in a crystal structure, changes in kinetic regime and/or passivation can cause splitting of voltammetric peaks.

*Chronoamperometry.* For irreversible reactions, the formal kinetics of the reaction at a constant potential is considerably more simple than in any potentiodynamic measurement. The time dependence of the reaction rate can easily reveal phenomena like passivation, nucleation of new reactive surfaces, electrochemically promoted dissolution, thin layer behaviour and other phenomena interpreted in general terms of heterogeneous reactions of solids. For example, with compact CuS electrodes, passivation and solid-state diffusion as the rate-determining steps were clearly proved<sup>28</sup>. Gervasi

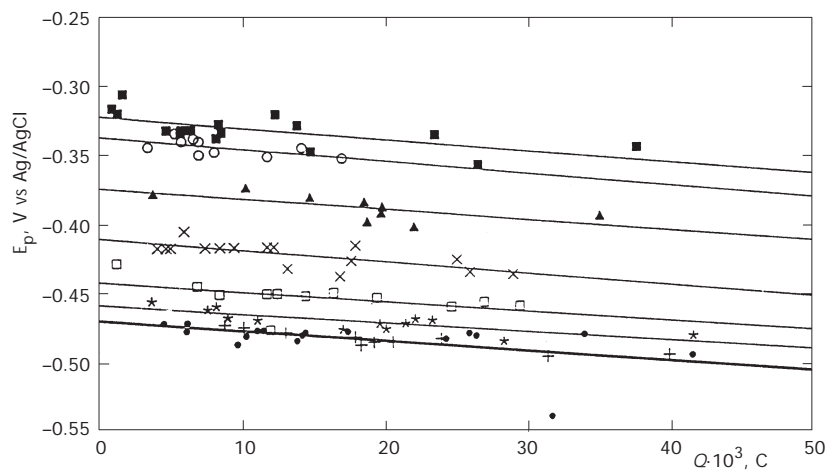


FIG. 2

Dependence of the voltammetric peak potential on the amount of electroactive compound in voltammetry of microparticles (Cu chalcogenides<sup>127</sup>): ● CuSe, + CuSe<sub>0.8</sub>S<sub>0.2</sub>, \* CuSe<sub>0.6</sub>S<sub>0.4</sub>, □ CuSe<sub>0.4</sub>S<sub>0.6</sub>, × CuSe<sub>0.3</sub>S<sub>0.7</sub>, ▲ CuSe<sub>0.2</sub>S<sub>0.8</sub>, ○ CuSe<sub>0.1</sub>S<sub>0.9</sub>, ■ CuS

*et al.*<sup>98,99</sup> also used chronoamperometry to study kinetics and mechanism of the passivation of Co electrodes. An overview of kinetic functions suitable for chronoamperometric data processing is available in ref.<sup>95</sup>.

*Charge (Q) and peak current ( $I_p$ ) in voltammetry.* The overall charge passed through the working electrode due to an electrochemical reaction is directly proportional to the actual amount of reactant involved in the reaction according to the Faraday law. However, less than the whole amount of solid present in the working electrode will in general be involved in the reaction.

Actually  $I_p$  depends on the peak shape. Both  $I_p$  and  $Q$  can hence only be used for quantitative analysis, provided calibration curves have been constructed. The requirement for calibration plots is especially essential in differential pulse voltammetry and other alternating current techniques if the voltammetric peaks are overlapped<sup>103,104</sup> and if the peak assignment is not clear<sup>105</sup>. The problem of calibration curves was avoided<sup>106</sup> by the method of "internal standard" in analysis of  $\text{Ag}_2\text{O}$  admixture in  $\text{AgO}$ , which was in fact normalisation of the minor  $\text{Ag}_2\text{O}$  signal to the sum of signals of major (matrix)  $\text{AgO}$  and  $\text{AgO}$  formed from  $\text{Ag}_2\text{O}$  by oxidation. This approach is similar to analysis of bulk stoichiometry described in Part 5.3.3. In the study of  $\text{Fe}_2\text{O}_3$  content in paleosoils, Grygar and van Oorschot<sup>107</sup> added a known amount of  $\text{MnO}_2$ , which yielded voltammetric peaks well separated from those of  $\text{Fe}_2\text{O}_3$ . The quantity was evaluated from the charge ratio between the peaks of  $\text{Fe}_2\text{O}_3$  and  $\text{MnO}_2$ . This approach could also overcome the drawback of VMP due to the unknown actual amount of a sample deposited on the electrode and/or involved in the electrochemical reaction. Charges of voltammetric peaks and chronocoulometry are best suited to analyses of stoichiometry of inorganic compounds, which under certain circumstances do not require calibration plots (Part 5.3.3.).

*Formal charge-transfer coefficient  $\alpha$ .* To estimate  $\alpha$  of a bulk solid, stationary polarisation curves are evaluated plotting logarithm of stationary current against potential; the estimate is based on a constant surface area of the reacting solid and hence is inapplicable to particulate solid, whose surface is changing in the course of experiment. The formal charge-transfer coefficient of powder can be estimated indirectly from the dependence of the peak potential on scan rate<sup>40,59,106,108</sup>, by analysis of the rising portion of voltammetric peaks<sup>109</sup>, or directly by potential-pulse chronoamperometry<sup>110,111</sup>.  $\alpha$ - $E_p$  plots were used by Doménech-Carbó *et al.*<sup>59</sup> to distinguish basic carbonates (malachite, azurite), acetate (verdigris), hydroxy chloride ( $\text{Cu}_2(\text{OH})_3\text{Cl}$ ), and copper resinate pigments, yielding voltammetric curves with similar peak potentials. The formal charge-

transfer coefficient is related to properties of the electrode<sup>39</sup>, reaction mechanism<sup>40</sup>, and phase composition and crystallinity of the sample<sup>59,112</sup>.

### 5.2. Reproducibility and Detection Limits

Voltammetry of solids has mainly been used for identification and analysis of stoichiometry of pure substances, but it was also proposed for quantitative analysis of mixtures<sup>2,13,103</sup>. The reproducibility of  $I_p$  and  $Q$  evaluations generally worsens going from pure electroactive substances through mixtures of pure electroactive substances to mixtures of electroactive substances in an inert matrix. The best reproducibility is achieved in the determination of stoichiometry of pure substances from relative values of charges, because they do not depend on the actual amount of the electroactive solids. Relative deviations <5% were reported for analysis of  $\text{Cu}_x\text{S}$  stoichiometry by Lamache and Bauer<sup>113</sup> and Brage *et al.*<sup>114</sup> and only about 1% for the Bi–Cu–Pb ratio in high-temperature superconductors by Scholz and Lange<sup>115</sup>.

The analysis of mixtures of pure electroactive solids requires equal properties of the mixture components necessary for their equal deposition on the electrode in VMP, equal reaction depth in CPEE with conducting binder and equal charge yield in CPEE with conducting binder; this has not been appropriately studied. The information on reproducibility of electroanalysis of solid mixtures is also rather rarely available. Relative standard deviation of  $\text{Cu}^0$  determination was found to be 4–8% by Gruner *et al.*<sup>38</sup> for the optimised carbon paste electrode, but the reproducibility was much worse for the other paste electrodes studied. In VMP of various artificial binary mixtures of electroactive components with calibration plots, relative standard deviation ranged from 3 to 15% according to Scholz *et al.*<sup>103</sup>.

The detection limits in voltammetry of solid reactants have been published only in a few cases. According to Brainina and Vydrevich<sup>13</sup>, in CPEE with non-conducting binder, the lowest estimate of the detection limit is given by the actual amount of particles of the analyte on the surface layer of the paste electrode, which is accessible from the solution of supporting electrolyte. They estimate the detection limit of 0.02% for 10  $\mu\text{m}$  analysed particles uniformly distributed in the paste electrode of 1-cm diameter, assuming access to 10 particles as a minimum amount for a reliable detection of the current. This limit was in accordance with experimental results for the determination limit of Ag admixtures in  $\text{Ag}_2\text{O}$  matrix. Brainina and Vydrevich believed that the detection limit in CPEE with conductive binder should be even lower due to a bigger amount of material available for reac-

tion. As low as 0.008% Mn was detected in calcium carbonate matrix by Komorsky-Lovrić *et al.*<sup>116</sup> using VMP. The detection limit of  $\text{MnO}_2$  and  $\text{Fe}_2\text{O}_3$  in artificial mixtures with  $\text{SiO}_2$  of the order of 0.1% was estimated by Grygar and van Oorschot<sup>107</sup> in VMP.  $\text{Fe}_2\text{O}_3$  signal was probably enhanced by some catalytic reaction that compensated the large background current in the respective potential range. Using CPEE with a conducting binder<sup>117</sup>, the determination limit of free ferric oxides in clay samples is of the order of 0.001%. Zejničović *et al.*<sup>118</sup> estimated the detection limit of 0.8% for an admixture of the less noble component in a compact electrode of the metal alloy. This detection limit also includes the matrix effect of the base alloy component yielding a neighbouring dominant voltammetric peak.

### 5.3. Examples of Electroanalysis of Inorganic Solids

The sample amount necessary for analysis in VMP or film electrodes can be lower than a milligram and quantitative analysis, in some cases, does not require any reference compounds. Long-range ordering in solid is required to diffract X-rays, and hence practically no meaningful signal can be obtained by XRD from amorphous phases. This fact also complicates a reliable quantitative XRD analysis of crystalline analytes in an amorphous matrix. On the other hand finely particulate samples, including nanocrystalline or amorphous phases, are rather advantageous for electrochemical analysis due to their high reactivity. In many cases, voltammetry integrates both sensitivity to elemental and phase composition, which can otherwise be only achieved by combination of two different techniques, *e.g.* XRD and electron-microprobe analysis. For example, five different Cu copper pigments, mainly basic salts, were distinguished by voltammetry of 0.1-mg microsamples from works of art; electron microprobe analysis is only able to identify Cu in the samples<sup>58</sup> and XRD is impossible with small samples. All these facts substantiate the effort of electrochemists to develop alternative approaches to analysis of solids. Analytical applications of electrochemical study of solids are summarised in Table II. In the next paragraphs, typical classes of analytical tasks are discussed.

#### 5.3.1. Elemental and Phase Analysis

Alloys, chalcogenides and other compounds containing electrochemically active elements such as Ag, Cu, or Pb, or compounds like Mn oxides have been frequently studied by voltammetry of solids. As  $\text{MnO}_2$  polymorphs exhibit different voltammograms for  $\text{H}^+$  insertion in neutral or alkaline solu-

TABLE II  
Papers devoted to electrochemical analysis of inorganic solids

Analyte	Task	Technique	Refs
Metals and alloys	Ag-Cu alloys	VMP	119
	Cu, determination	CPEE	38
	Dental alloys	VMP	120, 121
	Fe, reactivity of powders	VMP	122, 123
	Pb-Sb, elemental analysis	VMP	18
	Sn-Bi	VMP	124
Inorganic pigments (oxides, chalcogenides)	Identification	VMP	93, 125
	Identification	FE <sup>b</sup>	57, 58
Chalcogenides	Cu sulfides, stoichiometry	CPEE	113, 114
	Cu <sub>2-x</sub> Se, stoichiometry	CPEE	126
	CuSe <sub>x</sub> S <sub>1-x</sub> stoichiometry	VMP	127
	Pb-Sb sulfides, stoichiometry	VMP	19
	Various minerals	VMP	128, 129
Ag oxides	Ag <sub>2</sub> O-AgO mixture	CPEE	130
Ba, Sr, Pb chromates	Granulometry	CPEE	131-133
Cu oxides	CuO-ZnO catalysts		69
	HTSC <sup>a</sup> identification of phases, redox centres	VMP	134, 135
	Pigments and weathering products in works of art	FE <sup>b</sup>	58, 59
	Fe <sub>2</sub> O <sub>3</sub> , granulometry	CPEE	44, 94, 136
Fe oxides	NaFeO <sub>2</sub> and LiFeO <sub>2</sub> , granulometry	CPEE	137, 138
	Analysis of mixtures of $\alpha$ - and $\gamma$ -FeOOH	VMP	104
	Amorphous impurities in $\alpha$ -FeOOH	VMP	112
	Fe <sub>2</sub> O <sub>3</sub> and FeOOH in paleosoils	VMP	107
	Free Fe(III) oxides in clays	CPEE	117
	Pigments in works of art pieces	CPEE	105, 109
	Molecular sieves	CPEE	139,
Mn oxides	Mn in natural carbonates	VMP	116
	Mn in sediments	VMP	140
	Battery materials	VMP	74
	MnO <sub>x</sub> in archaeological glass	FE <sup>b</sup>	60
	Comparison of various Pb oxides	CPEE	141
Pb oxides	Glazes with Pb oxides	various	56
	Catalysts	CPEE	142
Pt compounds	Speciation of framework Ti <sup>4+</sup>	CPEE	143-146
Ti in zeolites	Distinguishing $\alpha$ - and $\beta$ -SnO <sub>2</sub>	CPEE	147
Sn oxides	Speciation of V in heterogeneous system VO <sub>x</sub> /TiO <sub>2</sub> (rutile)	SC <sup>c</sup>	148

<sup>a</sup> HTSC, high-temperature superconductors; <sup>b</sup> FE, polymer film electrode; <sup>c</sup> SC, single crystal electrode.

tions<sup>96,149</sup>, the reaction has been recently used for electrochemical analysis of Mn-oxide weathering products on archaeological glass samples<sup>60</sup>. On the other hand, Fe oxides yield usable electrochemical signals, although Fe is rather a less common subject of electroanalysis. In the case of Fe oxides, the phase specificity of the chemical reductive dissolution is traditionally used to determine the content of amorphous impurities in crystalline oxides (extraction with dithionite-citrate-hydrogencarbonate or oxalate solutions). A similar determination can be done by voltammetry<sup>112</sup>, which is, however, much less laborious than the traditional chemical route. Also oxidative dissolution of Cr oxides has a significant phase specificity, which was first visualised by voltammetry<sup>110</sup>. Another class of phases with particularly well-defined electrochemistry is that of metal chalcogenides<sup>19,128,129</sup>.

### 5.3.2. Solid Solutions

Solid solutions of isostructural compounds play an important role in material science. Solid solutions are crystalline phases with one or more sub-lattices containing two or more elements in ranges varying within a continuous interval. Solid solutions can be represented by general formula  $A_{1-x}B_x$  (alloys) or  $A_{1-x}B_xC$ , where A, B, and C are elements or units common to the whole series. The end members AC and BC may not be accessible, such as the members with  $x \approx 0$  in the series  $Li(Mn_{1-x}Fe_x)_5O_8$ . The basic structural features and electrochemical behaviour of solid solutions are summarised in Fig. 3. Miscibility of AC and BC is routinely evaluated by comparison of changes in the lattice parameters on varying  $x$ . In many cases such dependence is ordinarily linear according to the empirical Vegard rule<sup>150</sup>. Any discontinuities in the lattice parameters or even

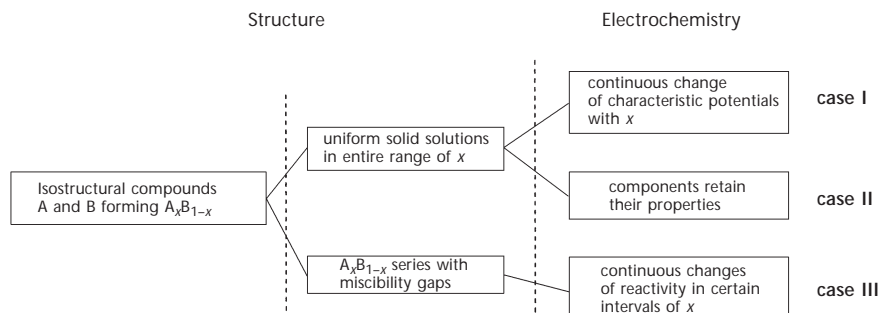


FIG. 3  
Basic relationship between structural and electrochemical properties of solid solutions

changes in the crystal symmetry or other departures from structural similarities are interpreted as miscibility gaps.

From an electrochemical point of view, it makes sense to distinguish the following three cases of solid solutions (the asterisk indicates the electroactive centre): (i)  $A_{1-x}B_xC^*$ , (ii)  $A^*_{1-x}B_xC$ , and (iii)  $A^*_{1-x}B^*xC$ . Examples of case (i) are  $AgCl_{1-x}Br_x$  and  $CuS_{1-x}Se_x$ , where silver and copper ions are electroactive and the anions are of a mixed composition, and also  $Ni_{1-x}Fe_x$  hexacyanoferates and  $Cu_{1-x}Fe_x$  hexacyanoferates, when the hexacyanoferate ions (with low-spin  $Fe^{2+}/Fe^{3+}$ ) are studied as electroactive centres. However, the latter two examples fall also into case (ii) with respect to the high-spin Fe ions that are substituted by nickel or copper, because these high-spin iron ions are also electroactive in a separate potential range. An example of case (ii) is nickel (hcf)<sub>1-x</sub>(hcco)<sub>x</sub> (hcf is hexacyanoferrate and hcco is hexacyanocobaltate), where only the hexacyanoferrate ions are electroactive. In the reductive dissolution of transition metal oxides,  $Fe^{III}-M^{III}$  oxides ( $M = Al, Cr$ ) are examples of case (ii) and  $Fe^{III}-Mn^{III,IV}$  oxides of case (iii). Examples of solid solutions studied by electrochemical means are shown in Table III.

In **case I** electrochemically reversible and irreversible reactions should be distinguished. In the reversible case  $I_R$ , electroanalytical measurements are well suited to obtain information on their composition and thermodynamics, because the  $E_p-x$  function is of thermodynamic nature. The thermodynamics of mixed phases allows answering two vital questions when electrochemical techniques are applied to these systems:

1. Is a given material a solid solution or is it just a mechanical mixture of two phases?

2. If it is a solid solution, what is its composition?

Figure 4 depicts the electrochemical signals of two pure phases A and B and that of a solid solution  $A_xB_{1-x}$ . When the material to be studied is a mechanical mixture of the two phases A and B then two separate signals result. The signals depicted in Fig. 4 may be those of an electrochemical reduction or oxidation, and they may be measured by any voltammetric technique, *e.g.* linear-scan voltammetry or a pulse technique, as long as the characteristic potentials of the used technique are unequivocally depending on the formal potentials of the electrochemical system. In any case, it is necessary to study also samples of the pure compounds A and B. When  $E_A$  and  $E_B$  are the characteristic potentials of these pure compounds, then it follows that the characteristic potential  $E_{AB}$  of the solid solution  $AB_x$  with the molar ratio  $x_B = n_B/(n_A + n_B)$  will shift with the molar ratio as follows:

$$E_{AB} = E_A + x_B (E_B - E_A) - \frac{RT}{zF} [(x_A \ln x_B + x_B \ln x_B) - x_A x_B \varepsilon]. \quad (5)$$

The term  $(RT/zF)(x_A \ln x_A + x_B \ln x_B)$  represents the deviation from linearity caused by the mixing entropy, and the term  $(RT/zF)x_A x_B \varepsilon$  is due to a possible non-ideality of the solid solution system ( $\varepsilon$  is a parameter for the non-ideality). The mixing entropy adds rather little to the non-linearity of the dependence of  $E_{AB}$  on  $x_B$ . It just amounts to  $-17.7$  mV for  $x_B = x_A = 0.5$ ,  $T = 25$  °C and  $z = 1$ . When the reversibility of the electrochemical processes in the pure phases and the mixed phases differ, further deviations from Eq. (5) must be expected.

Copper(II) sulfide and selenide form a continuous series of solid solutions Cu(S,Se) (Meyer *et al.*<sup>127</sup>). Mechanically immobilised on a graphite electrode, the pure compounds and the solid solutions can be reduced to metallic copper and the sulfide and selenide ions are liberated and possibly protonated (depending on the pH of the solution).

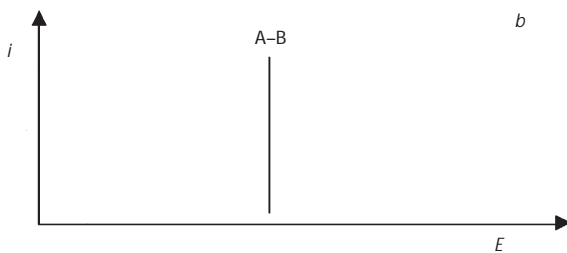
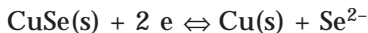
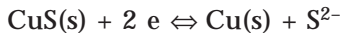


FIG. 4  
Peak positions of single electroactive compounds A, B (a) and their solid solution  $\text{A}_x\text{B}_{1-x}$  (b)

Figure 5 depicts the linear sweep voltammograms for the reduction of the pure phases CuS and CuSe, and of the solid solution  $\text{CuSe}_{0.4}\text{S}_{0.6}$ . The voltammogram of the solid solution  $\text{CuSe}_{0.4}\text{S}_{0.6}$  exhibits a single peak, in accordance with the expectations of mixed phase thermodynamics. For an exact determination of the composition of the solid solution from a measurement of the peak potential, an empirical calibration is necessary, using a set of samples of known composition. Further, it is necessary to establish in preliminary experiments whether the peak potential depends significantly on the amount of particles immobilised on the electrode surface. This feature depends very much on the substances. In the case of the copper selenides and sulfides, this dependence has to be taken into account. When each sample is measured several times on varying its amount, one can plot the dependence of the peak potentials on the actual charges that are proportional to the amount of the reduced substance (Fig. 2). In the studied case the  $E_p$ - $Q$  functions are all linear and parallel, and one can extrapolate the peak potentials *versus* the molar ratio  $x_{\text{Se}}$  gives a smooth curve that can be used as a calibration plot for the analysis of samples of unknown composition (Fig. 6).

Case  $I_{\text{IRR}}$  has not been sufficiently well described; the smooth dependence of peak potentials on elemental composition must have kinetic reasons. The examples of Fe-Mn oxide dissolution<sup>154–156</sup> are shown in Table III. Voltammetric peak potentials of irreversible reductive dissolution of the

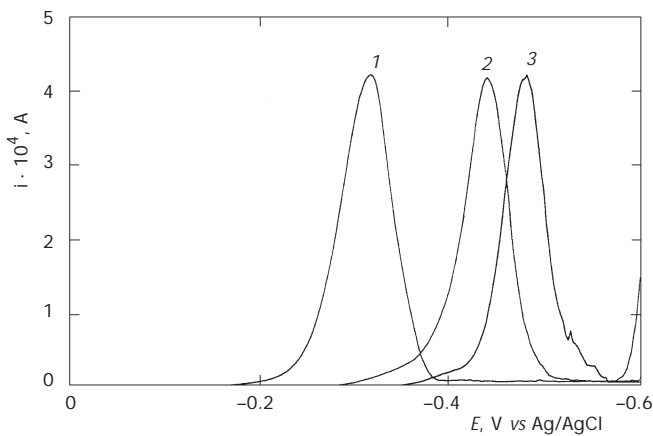


FIG. 5  
Voltammetric curves of 1 CuS, 2  $\text{CuSe}_{0.4}\text{S}_{0.6}$  and 3 CuSe (ref.<sup>127</sup>)

TABLE III  
Papers devoted to electrochemical analysis of solid solutions

Case <sup>a,b</sup>	Solid solution	Example and topic of study	Refs
I <sub>R</sub>	Isostructural with continuous change of properties	AgCl-AgBr, CuSbS <sub>2</sub> /CuBiS <sub>2</sub> , thermodynamics Cu <sub>2</sub> Se-Cu <sub>2</sub> S, thermodynamics Fe(III)/Ni(II) hexacyanoferrate Fe(III)/Cu(II) hexacyanoferrate	151 127 152 153
I <sub>IRR</sub>	Isostructural with continuous change of properties	C-(Mn <sub>1-x</sub> Fe <sub>x</sub> ) <sub>2</sub> O <sub>3</sub> and Ca-Fe-Mn-O perovskites, reductive dissolution, uniformity of synthetic samples Li-Fe-Mn-O spinels, uniformity of synthetic samples	154
II	Isostructural	LiM <sub>x</sub> Mn <sub>2-x</sub> O <sub>4</sub> , 5 V Li <sup>+</sup> electrodes	157-162
III	Isostructural with miscibility gaps	LiMn <sub>2</sub> O <sub>4</sub> - $\lambda$ -MnO <sub>2</sub> , Li <sup>+</sup> selective electrode LiMn <sub>2</sub> O <sub>4</sub> - $\lambda$ -MnO <sub>2</sub> , Li <sup>+</sup> batteries LiNiO <sub>2</sub> -Li <sub>1-x</sub> NiO <sub>2</sub> , Li <sup>+</sup> batteries	67 163, 164 165, 166

<sup>a</sup> See Fig. 3. <sup>b</sup> Subscript R stands for electrochemically reversible reactions driven by thermodynamic equilibria, IRR for irreversible reactions driven by heterogeneous kinetics.

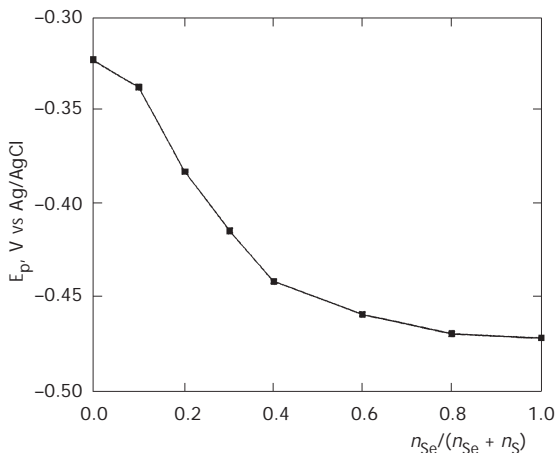


FIG. 6  
Voltammetric peak potentials of solid solution CuS<sub>x</sub>Se<sub>1-x</sub> (ref.<sup>127</sup>)

samples with structure of defective (O-deficient) perovskite  $\text{Ca}_3(\text{Fe},\text{Mn})_3\text{O}_8$  and cubic Fe-substituted bixbyite (cubic  $\text{Mn}_2\text{O}_3$ ) smoothly depend on  $\text{Fe}/(\text{Fe}+\text{Mn})$  (Grygar *et al.*<sup>154</sup>). Voltammetry using reductive dissolution of Li-Fe-Mn-O ternary spinels<sup>155</sup> and voltammetry combined with powder XRD analyses and Curie temperature measurements<sup>156</sup> identified two compositional regions of uniform solid solutions and one region of uncertain uniformity. Electrochemical reductive and oxidative dissolution of Fe-Cr mixed oxides is an example of  $\text{A}_x\text{B}_{1-x}\text{C}$  where only A (Fe in reductive dissolution) or only B (Cr in oxidative dissolution) is electroactive<sup>167</sup>. Such combination leads to passivation at growing content of the component that is inactive in a given type of redox dissolution.

In **case II**, the electroactive ions A and B retain their original electronic properties and hence behave electrochemically as a mixture of AC and BC, although structurally  $\text{A}_{1-x}\text{B}_x\text{C}$  is a uniform solid solution. This behaviour is responsible for two plateaus in charge/discharge curves of  $\text{LiM}_x\text{Mn}_{2-x}\text{O}_4/\text{M}_x\text{Mn}_{2-x}\text{O}_4$ , that was explained by separated redox alteration of  $\text{M}^{\text{III}}/\text{M}^{\text{IV}}$  and  $\text{Mn}^{\text{III}}/\text{Mn}^{\text{IV}}$  ( $\text{M} = \text{Cr}$  (refs<sup>157–159</sup>),  $\text{M} = \text{Fe}$  (refs<sup>159,160</sup>),  $\text{M} = \text{Co}$  (refs<sup>159,161</sup>),  $\text{M} = \text{Ni}$  and  $\text{Cu}$  (ref.<sup>159</sup>)). The studies showed that redox cycling of both Mn and M metals occurs during a complete charge/discharge reaction. Electron energy loss spectroscopy proved that  $\text{Cr}^{\text{III}}$  is oxidised to  $\text{Cr}^{\text{IV}}$  (Sigala *et al.*<sup>157</sup>) and Mössbauer spectroscopy that  $\text{Fe}^{\text{III}}$  is oxidised to  $\text{Fe}^{\text{IV}}$  (Ohzuku *et al.*<sup>162</sup>) in the step at a more positive potential. The uniformity of Li-Fe-Mn-O spinel solid solutions was proved by Grygar *et al.*<sup>156</sup>, and only a minor deviation from the Vegard rule was found in the  $\text{Li}_2(\text{Co}_{1-x}\text{Mn}_{3+x})_2\text{O}_4$  series, without a direct prove of segregation of the metal ions in the crystal lattice<sup>161</sup>.

Due to the sensitivity of the electrochemical reactivity, it is not surprising that in **case III** the structural discontinuity causes double (split) voltammetric peaks, double (multiple) plateau on discharge curves or other features occurring regularly at a given value, as in  $\text{Li}^+$  extraction from  $\text{LiMn}_2\text{O}_4-\lambda\text{-MnO}_2$ . Although the end members are isostructural cubic spinels, an abrupt change in reaction rate is observed at  $x \approx 0.5$ , causing a current minimum between two overlapping peaks in the reaction (6)



Although this phenomenon was reported already in the first papers dealing with this system<sup>168</sup> and since then it has been studied by numerous au-

thors, the structural discontinuity in the solid solution  $\text{LiMn}_2\text{O}_4-\lambda\text{-MnO}_2$  was proved by diffraction studies only in 1998 (refs<sup>163,164</sup>). Similarly complex is the course of electrochemical  $\text{Li}^+$  insertion/extraction in the system  $\text{Li}_{1-x}\text{NiO}_2$  in which, at certain  $x$ , structural discontinuities due to Li ordering cause stepped discharge curves<sup>165,166</sup>. Also in that case, voltammetry is more sensitive to structural discontinuities than for example XRD.

In several reported cases voltammetry was more suitable than XRD for characterisation of elemental composition of solid solutions, mainly due to poor sample crystallinity and/or small lattice changes with  $x$  (CuFe hexacyanoferrates<sup>153</sup>, Fe-Mn oxides<sup>154,155</sup>). Voltammetry can hence detect non-uniformity in elemental distribution in synthetic samples<sup>156,167</sup>.

### 5.3.3. Stoichiometry of Metal Oxides and Chalcogenides

Sapozhnikova *et al.*<sup>169,170</sup> proposed to examine the anodic voltammetric peaks of Cu-Fe-O and Cu-Li-Fe-O spinels to evaluate the actual valences of the metal ions, using calibration curves constructed from the currents at the potentials corresponding to the redox changes of the ions. However, this approach was only suitable for qualitative characterisation. On the contrary, stoichiometry can be calculated from charge ratios in voltammetric curves which are very reliable in voltammetry of solids, assuming that a constant amount of samples is involved in all redox reactions. Such case was the analysis of stoichiometry of copper sulfides  $\text{Cu}_x\text{S}$  that belongs among the first important reports on direct electroanalysis of solids<sup>113</sup>.  $\text{Cu}_x\text{S}$  sulfides yield chemically reversible reaction (7).



The reaction proceeds via intermediates  $\text{Cu}_{2-\delta}\text{S}$  with  $\delta = 0.08, 0.33, 0.40$ , and 0.69. At slow scan rates, the formation of intermediates is responsible for partly overlapped voltammetric peaks whose charges can be used for stoichiometry calculation. As Lamache and Bauer<sup>113</sup> used CPEE with an aqueous solution as binder, all  $\text{Cu}^{2+}$  formed on oxidation was available for the reverse reaction. Copper selenides  $\text{Cu}_x\text{Se}$  were characterised in a similar manner<sup>126</sup>.

Stoichiometry of As, Sb, and Sn sulfides and sulfur salts of Tl, Sn, Pb, and Ag was studied by Zhang *et al.*<sup>120</sup>. For example, the charges of the reduction of  $\text{Tl}_2\text{S}$ ,  $\text{TiS}$ ,  $\text{Ti}_4\text{S}_3$  and  $\text{Ti}_2\text{S}_5$  to  $\text{Tl}^0$  and  $\text{S}^{2-}$  were compared to the charge of

subsequent oxidation of  $\text{Tl}^0$  to  $\text{Tl}^{3+}$ , which permitted to distinguish these phases reliably. Zhang *et al.* used VMP methodology; neither the amount of sample on the electrode nor the amount of  $\text{S}^{2-}$  evolved in pre-electrolysis were necessary to be known for such analysis.

Scholz and Lange<sup>115</sup> determined stoichiometry of high-temperature superconductors  $\text{Bi-Pb-Sr-Ca-Cu-O}$ , using charges obtained by anodic stripping voltammetry of Bi, Cu, and Pb after a preliminary cathodic pre-electrolysis. The peak separation was improved by sample mixing with  $\text{Hg}_2\text{Cl}_2$  before the pre-electrolysis. The accuracy of the determination of Cu, Bi, and Pb was 1.6%.

### 5.3.4. Identification/Characterisation of Redox Centres in Solids, Redox-Based Speciation in Solid State

Solid-to-solid transformations can yield voltammetric peaks that reveal the presence of structurally different redox centres in inorganic solids. This phenomenon has been demonstrated in numerous cases of compounds containing electroactive metal ions in two different coordination environments, *e.g.* in octahedral and tetrahedral sites in the oxide framework ( $\text{Ti}^{n+}$  in zeolite samples<sup>143,144</sup>) or with different neighbouring ions in the same coordination polyhedrons ( $\text{Mn}^{\text{III,IV}}$  in  $\text{MnO}_2$  polymorphs todorokite and hollandite<sup>139</sup>).

An impressive example of the sensitivity of voltammetric measurements to the coordination environment of redox centres in solids is the cyano-metallates. Three kinds of metals can be distinguished in the (mostly) cubic lattice, all with octahedral coordination: framework ions coordinated to C, framework ions coordinated to N, and ions in the interstitial cavities<sup>2</sup>. When the metal ions coordinated to nitrogen and carbon are electrochemically active, their redox potentials allow a clear designation of the coordination. For example C- and N-coordinated ions  $\text{Cr}^{3+}$  yield two voltammetric peaks with almost 2 V separation<sup>171</sup>. The interstitial ions are usually alkali metal ions; their involvement in electrochemical reactions of the solid hexacyanometallates can only be deduced from the dependence of the formal potential of the redox system on the activity of these ions in aqueous solution. The experimentally found relations between the formal potentials of solid hexacyanometallates and the ion potentials and lattice constants have been previously published<sup>172</sup>; however, only recently these relations could also be theoretically derived<sup>173</sup>.

Voltammetry was also used to study the nature of bonding of ions in the zeolite ion-exchangeable positions or in their framework.  $\text{Ag}^{\text{I}}$  (refs<sup>52,174,175</sup>),

$\text{Cu}^{\text{II}}$  (refs<sup>176,177</sup>), and  $\text{V}^{\text{V}}$  (refs<sup>178,179</sup>) coordinated in different environments of a zeolite structure exhibit different behaviour and also differ with respect to dissolved free ions. The small but definite energy differences between the ions with different coordination in zeolite are responsible for the set of overlapped voltammetric peaks. For example, nine  $\text{Ag}^{\text{I}}$  species were identified in  $\text{Ag}^+$ -exchanged zeolite 4A by Li and Calzaferri<sup>52</sup>.  $\text{Ti}^{\text{IV}}$  was found to be reducible when incorporated in the zeolite framework (coordination number 4) but not in ion-exchangeable positions or in free  $\text{TiO}_2$  (coordination number 6, refs<sup>143,144</sup>). Even though another interpretation of the electrochemical speciation of Ti in Ti-modified zeolite (silicalite) has been reported by Bodoardo *et al.*<sup>146</sup>, the difference between tetra- and octa-coordinated Ti has been confirmed. Speciation of Ti in zeolites was also studied by Doménech *et al.*<sup>145</sup> who found voltammetry to be sensitive to differences in tetracoordinated Ti ions with different number of OH and silanol groups.

$\text{Cu}^{n+}$  ions in oxides of various compositions also exhibit various electrochemical behaviour. Voltammograms of  $\text{YBa}_2\text{Cu}_3\text{O}_{7-\delta}$  deviated for different  $\delta$ , *i.e.* different valence and/or coordination of Cu ions in the crystal lattice<sup>134,135,180,181</sup>.

Reversible redox reactions of  $\text{Mn}^{\text{IV}}$  were used by De Guzman *et al.*<sup>139</sup> for characterisation of  $\text{MnO}_2$ -based molecular sieves of different crystal structures, hollandite and todorokite. Both these phases are composed of infinite chains of edge-sharing octahedra forming 3D structure with  $2 \times 2$  and  $3 \times 3$  channels of missing octahedra. The channels contain alkaline and alkaline earth metal ions and hence the mean Mn valence in the oxides is below 4. Electrochemical cycling of  $\text{Mn}^{2+}$  in the structure of todorokite permits to distinguish these two phases.

### 5.3.5. Particle Size and Crystallinity

The morphology of particles is of great importance for the course of electrochemical dissolution reactions. The rate of these reactions is controlled by heterogeneous reaction kinetics or by diffusion of the reaction products as it is typical of irreversible dissolution reactions, or in the reaction kinetics in thermal analysis. The influence of particle size in voltammetry was explicitly mathematically expressed by Brainina and Vydrevich<sup>13</sup>, Brainina and Lesunova<sup>106</sup>, and Mouhandess *et al.*<sup>44,94,136</sup> in CPEE and by Grygar<sup>95</sup> in VMP. Voltammetric peak potentials of irreversible reaction of powder are directly proportional to logarithm of their particle size (Eq. (8)):

$$E_p = RT/(\alpha nF) \ln d + \text{const.}, \quad (8)$$

where  $\alpha$  is the formal charge transfer coefficient (Part 5.1.),  $n$  is the number of electrons exchanged in the rate-determining step, and  $d$  is the particle diameter, unless particle passivation or change of the kinetic regime occurs with increasing particle size. Such dependence is trivial in the heterogeneous kinetics of solid reactants and can be demonstrated by so-called shrinking-particle models describing a decrease in the overall reacting surface due to particle consumption. The linear dependence of peak potentials on the logarithm of a specific surface area was observed for Fe oxides<sup>100</sup> and LiMn<sub>2</sub>O<sub>4</sub> (ref.<sup>155</sup>). Extreme aggregation of particles by thermal treatment causes transformation of peaks into waves in the reductive conversion of Ba and Pb chromates<sup>131,132</sup> and Fe oxides<sup>44</sup>, while the sample grinding has the opposite effect.

Another phenomenon known from thermal analysis and dissolution kinetics, is that the wider the size distribution of reacting particles, the slower completing the dissolution reaction. Formally, the rate of this process for powder may be expressed by an increasing apparent reaction order  $\gamma$  (see the review by Burnham and Braun<sup>182</sup>). Also introducing reactivity distribution due to the presence of more unresolved species of different reactivity leads to increase of  $\gamma$  (Boudreau and Ruddick<sup>183</sup>, Postma<sup>184</sup>). In voltammetry the increasing  $\gamma$  means broader peaks or even their transformation to waves with a slow current decrease beyond the peak<sup>100</sup>. An alternative to introducing the formalism of the general reaction order is to approach the size distribution using a set of monodisperse particle-size classes and to model the voltammetric peak shape<sup>94</sup>.

Other non-trivial influences of the particle size on voltammetric curves of particulate solids cause that only a certain fraction of the reactant is converted during the first voltammetric scan and a slowly decreasing peak is repeatedly observed on subsequent scans<sup>38,44</sup>. A change in the reaction regimes or passivation can be the reason<sup>38</sup>. If TiC or big Cu particles are electrochemically dissolved close to the region of passivation, the resulting voltammetric peaks are flattened and the peak potential is shifted<sup>38</sup>. A similar tendency was observed for Fe particles<sup>122,123</sup>. Such a passivation behaviour becomes more pronounced for bigger particles and faster scan rates.

The presence of an amorphous or very poorly crystalline fraction, which is generally more reactive and yields prepeaks in both reversible (cyano-metallates<sup>82</sup>) and irreversible reactions (Fe oxides<sup>112</sup>) is another phenome-

non, causing a shift of  $E_p$  due to sample crystallinity. Each such case should be carefully evaluated prior to conclusions are drawn, because formally similar effects (*i.e.*, prepeak(s) with faster kinetics) occurring during the solid-to-solid reduction of  $\text{MnO}_2$  to  $\text{MnO}_{2-x}(\text{OH})_x$  were reported to be caused by a surface layer and/or chemisorbed oxygen<sup>96,97</sup>.

#### 5.4. Examples of Electroanalysis of Organic and Organometallic Solids

Solid-state reactions are a very important class of processes<sup>185</sup> playing a key role in many natural (mineralisation, corrosion, radiation-induced processes) and industrial processes (in ceramics, batteries, electrochromic materials, electrosynthesis, *etc.*). Although of considerable potential benefit, the solid-state reactivity of organometallic<sup>186</sup> and organic<sup>187</sup> materials when exposed to oxidising or reducing conditions, has been rarely explored. These materials are commonly studied in organic solvents, but the solid-state redox processes in the presence of (more important) aqueous solution environments remain unknown. There are several examples of studies (see Table IV) showing that important insight into solid-state redox processes can be gained from voltammetric experiments.

TABLE IV  
Selected papers devoted to the electrochemical analysis of organic and organometallic solids

Analyte	Task	Technique	Refs
$\text{C}_{60}$ fullerene	Study of ion insertion processes for energy storage	Evaporation	188
Cobalt phthalocyanine	Solid-state electrocatalysis	VMP	189
Cr metal complexes	Matrix stabilisation and detection of unstable intermediates	VMP	190
Decamethylferrocene	Solid-to-solid redox conversion	VMP	191
Indigo	Study of the redox dissolution process	VMP	91
Insecticide	Quantitative detection in cucumber	Evaporation	192
Metallocenes	Solid-state redox process	VMP	151
Mn complexes	Solid-state photoelectrochemistry	VMP	193
Ru metal complexes	Characterisation of fast ion insertion	VMP	79
TCNQ	Formation of cation insertion products as analytical tool	VMP	55

Compared to solid-state redox reactions of inorganic materials, there is little known about the solid-state electrochemistry of organic materials. The ability of some electroactive materials such as fullerene C<sub>60</sub> (Chlistunoff *et al.*<sup>188</sup>) or 7,7,8,8-tetracyanoquinodimethane (Suarez *et al.*<sup>86</sup>) to undergo chemically reversible electroinsertion of cations or anions, has been established over the recent years. However, the mechanistic understanding and predictability of these processes are still poor. Organic solid-state redox reactions driven by milling with a suitable reducing agent have been proposed<sup>187</sup> as interesting alternatives to conventional solvent-based organic processes. Little is known about similar but electrochemically driven processes and the industrial (chromate-mediated) electrooxidation of anthracene to anthraquinone<sup>194</sup> is the only example of an application of this class of processes.

Redox dissolution processes are important in vat dyeing. The prototypic reaction is the reduction of indigo to leucoindigo, which is then adsorbed on textile fibers and exposed to air. A study of the solid-state redox properties of indigo has been reported by Bond *et al.*<sup>91</sup>. In Fig. 7 a general reaction scheme for both oxidation and reduction of indigo is shown, together with corresponding cyclic voltammetric responses. Solid indigo was immobilised at the surface of a graphite electrode and immersed into a buffer solution. Voltammetric experiments as a function of solution pH and composition have been reported, during which three distinct types of processes were detected. Process A (see Fig. 7) has been identified as 2 electron-2 proton reduction of indigo at the surface of solid particles. Correspondingly, process B with a similar pH dependence was attributed to the 2 electron-2 proton interfacial oxidation of solid indigo. In contrast to processes A and B, process C underwent a shift towards less negative potentials upon decreasing the concentration of protons, and the current of this reduction peak increased upon rotation of the electrode (see Fig. 7). Therefore, process C has been identified as a process involving electroinsertion of cations followed by slow dissolution.

The redox reactivity of organic and organometallic solids has been explored for several model systems (*e.g.* Bond and Scholz<sup>151</sup>). An interesting aspect of these solid-state redox processes is the surprising ability of some materials to undergo a reversible and very fast electrochemically driven ion insertion<sup>195</sup>. Figure 8 shows the voltammetric responses observed for oxidation of a diruthenium complex immobilised at the surface of a graphite electrode as a PF<sub>6</sub><sup>-</sup> salt. Rapid anion-insertion processes were discovered for different types of anions and the effect of replacing Ru with Os was ex-

plored. The solid-state reaction has been monitored by *in situ* electrochemical confocal Raman spectroscopy.

It has been shown by VMP methods that the “matrix effect” in solid-state redox processes can have a considerable impact on the lifetime of unstable intermediates<sup>190</sup>. The carbonyl chromium complex  $[\text{Cr}(\text{CO})_2(\text{dppe})_2]$  (dppe is 1,2-diphenylphosphinoethane) (see Fig. 9) exists in cis and in trans configuration. The cis form is stable for the neutral metal complex. However, after one-electron oxidation in solution, *cis*- $[\text{Cr}(\text{CO})_2(\text{dppe})_2]^+$  rapidly isomerises to *trans*- $[\text{Cr}(\text{CO})_2(\text{dppe})_2]^+$ . Figure 9 shows the multicycle solid-state voltammogram obtained for the oxidation of solid *cis*- $[\text{Cr}(\text{CO})_2(\text{dppe})_2]$  in aqueous NaCl. Surprisingly, the isomerisation process is slowed down considerably. During the first potential cycle, a reduc-

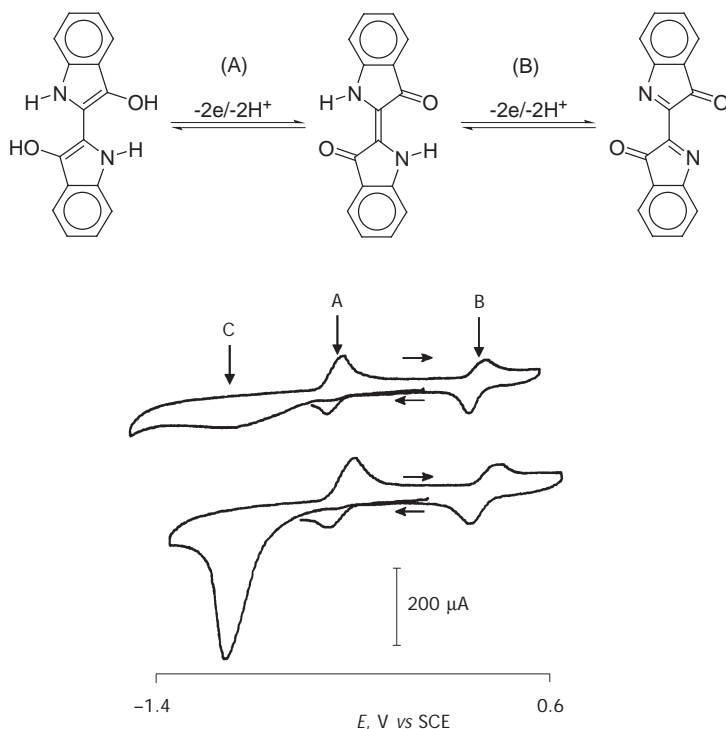


FIG. 7

General reaction scheme for the reduction and oxidation of indigo<sup>91</sup>. Cyclic voltammograms (scan rate  $0.2 \text{ V s}^{-1}$ ) obtained for indigo immobilised at a basal-plane pyrolytic graphite electrode (diameter of  $4.9 \text{ mm}$ ) and immersed in  $0.1 \text{ M}$  aqueous  $\text{NH}_4^+$ -Britton-Robinson buffer at pH 7. The first voltammogram was obtained for stagnant solution, the second one under rotating-disc electrode conditions (600 rpm)

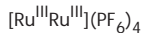
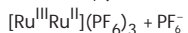
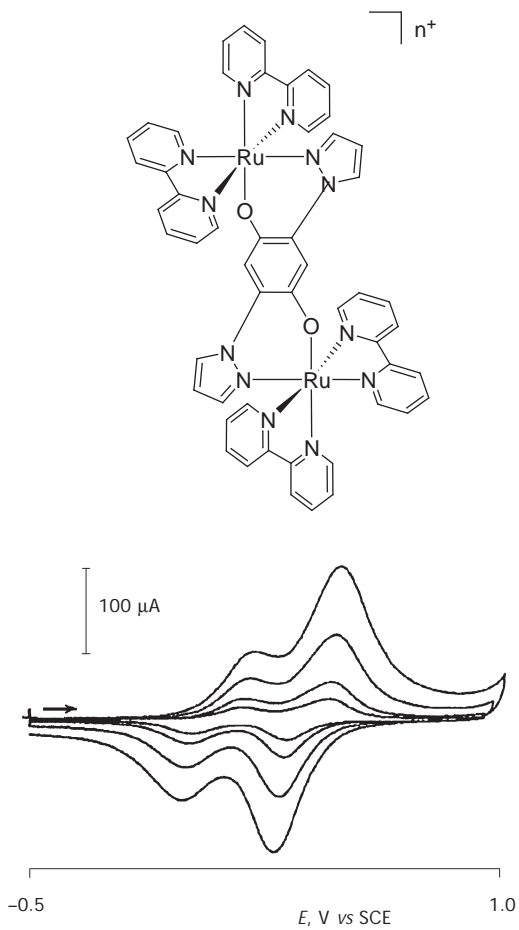


FIG. 8

Structure of a diruthenium complex employed in form of its  $\text{PF}_6^-$  salt for solid-state voltammetric experiments<sup>195</sup>. Cyclic voltammograms (scan rates of 100, 50, 20, 10  $\text{mV s}^{-1}$ ) for the oxidation of the solid diruthenium compound immobilised at a graphite electrode and immersed in aqueous 0.1 M  $\text{KPF}_6$ . The reaction sequence corresponding to the two oxidation signals is also shown

tion signal for the unstable intermediate is detected and, during continued cycling of the potential, the response of the *cis* isomer is decreasing, with the response of the *trans* isomer increasing simultaneously. An FTIR spectroscopic evidence for the unstable cationic *cis* complex has been reported.

Finally, mechanistic details for the electrochemical reduction and re-oxidation of TCNQ have been reported by several groups. In this model system, the importance of nucleation process can be proven by potential-step and cyclic voltammetric experiments. Figure 10 shows a typical voltammogram obtained for the solid-state reduction of TCNQ to  $\text{K}^+[\text{TCNQ}^-]$ . An inert zone between the signals for reduction and oxidation points to a considerable overpotential required for both processes. By reversing the scan direction at the foot of a voltammetric wave, very interesting mecha-

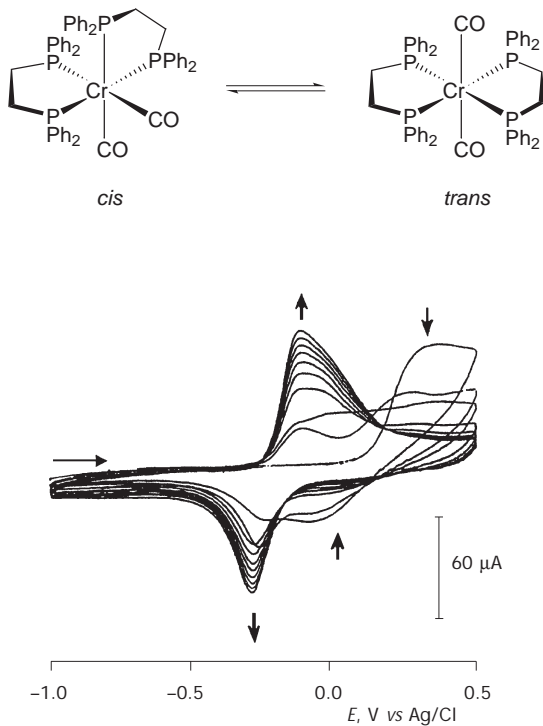


FIG. 9

Reaction scheme for the isomerisation of *cis*- to *trans*- $[\text{Cr}(\text{CO})_2(\text{dppe})_2]$  (ref.<sup>190</sup>). Multicycle voltammogram (scan rate  $0.2 \text{ V s}^{-1}$ ) for the oxidation of solid  $[\text{Cr}(\text{CO})_2(\text{dppe})_2]$  immobilised at a basal-plane pyrolytic graphite electrode (diameter of 4.9 mm) and immersed in 0.1 M aqueous NaCl at  $50^\circ\text{C}$

nistic conclusions can be drawn. The loop behaviour (Figs 10b and 10c) for both the reduction and reoxidation indicates that nucleation is required for both processes. Nucleation is responsible for the inert zone and the considerable overpotential observed for many solid-state electrochemical processes. For TCNQ-type processes, there are reaction intermediates preceding the  $\text{TCNQ}^-$  anions. However, due to the nucleation overpotential these thermodynamically allowed intermediates are inaccessible. Furthermore, an electrochemical solid-state transformation has been reported to lead to unusual solid phases obtained typically only at low temperatures<sup>89</sup>. This is another indication of non-equilibrium conditions during the electrochemical solid-state process.

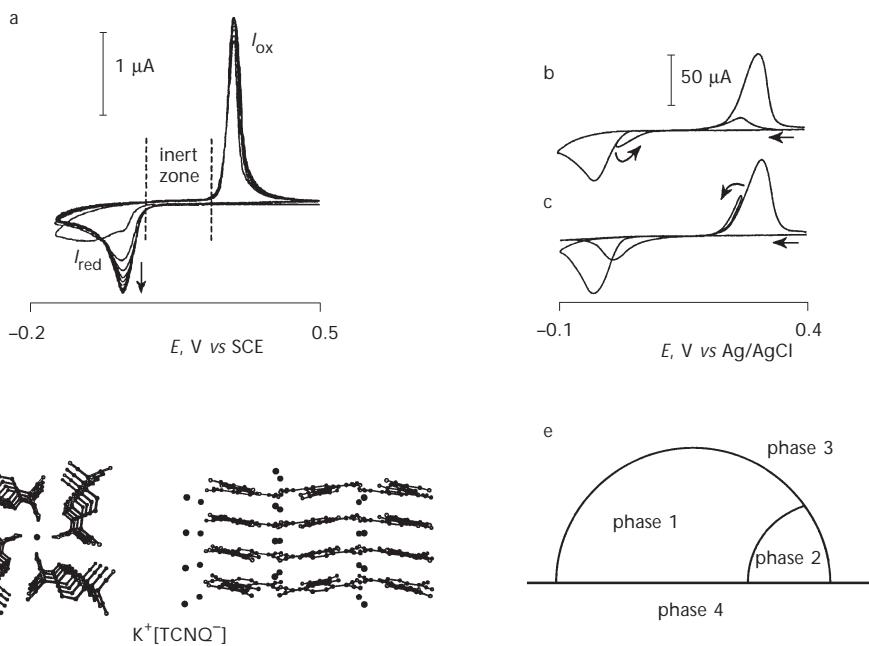


FIG. 10

a Development of the voltammetric response (scan rate  $0.1 \text{ V s}^{-1}$ ) of nanocrystals of TCNQ immobilised on a RAM electrode and immersed in aqueous  $0.1 \text{ M KCl}$  (ref.<sup>55</sup>). b Cyclic voltammograms (scan rate  $0.2 \text{ V s}^{-1}$ ) for nanocrystals of TCNQ immobilised on a  $1 \text{ mm}$  diameter Au electrode immersed in aqueous  $0.1 \text{ M KCl}$ . During the second cycle the potential is reversed at the foot of the reduction signal and a characteristic "loop" is indicated by the arrow. c Cyclic voltammograms obtained under conditions as in b, showing the characteristic "loop" also for the oxidation process. d Structural feature of  $\text{K}^+[\text{TCNQ}]$  showing the location of  $\text{K}^+$  in channels. e Schematic diagram indicating the presence of four phases during an electrochemical solid-to-solid transformation with nucleation

## 6. FUTURE PROSPECTS

The present state-of-art of electrochemical solid-state analysis fulfils requirements in many branches of chemistry and materials science, providing information on the thermodynamics of solids (formal potentials, stability constants<sup>127,151,196</sup>), identification and determination of elements and compounds of aliovalent metals, control of synthesised samples (phase purity, particle size, and uniformity<sup>112,154,156</sup>), etc. There have been a lot of examples since the 1990's that non-electrochemists adopted electroanalysis to solve problems of metal speciation and reaction mechanisms in chemistry, material science and mineralogy, showing the interdisciplinary scope of electrochemistry of solids.

The direct determination of stoichiometry and redox analysis of solids have proven to belong among the most accurate electrochemical analyses, as demonstrated by examples of metal chalcogenides in the 1970's (ref.<sup>113</sup>) and superconducting cuprates<sup>115</sup> in the 1990's. Electroanalysis of solids will remain a powerful tool for all compounds with their redox reactions as a substantial feature, such as redox catalysts<sup>145,148</sup> and inorganic pigments<sup>57,58,93,125</sup>.

Interrelations between electrochemical reactivity and structure of solids will be studied for a continuously growing number of organic and inorganic solids.

Amorphous and nanocrystalline solids and analytes in amorphous matrix, which limit application of XRD quantitative analysis, are rather advantageous for electrochemical analysis, because small particles retain remarkably well the electrochemical properties of larger crystals, as long as the size does not approach the atomic (molecular) range. However, comprehension of the relation between the electrochemical properties of solids and their order/disorder and particle size, in particular when approaching the molecular size range, still demands a lot of further experimental and theoretical studies.

Multicomponent and highly heterogeneous systems can be electrochemically analysed provided the target analyte is electroactive and present at levels  $> 0.1\%$  (ref.<sup>107</sup>) or sometimes even lower<sup>13,116,117</sup> that is at least by one order of magnitude better detection limit than that for powder XRD. Voltammetric analysis combines elemental and phase specificity for many compounds, which is advantageous for distinguishing mixtures of isostructural compounds and their solid solutions. This is especially valuable with respect to low amounts of sample needed for electrochemical analysis: routine phase identification has been done with samples of 0.1 mg (refs<sup>57,60</sup>).

## 7. REFERENCES

1. Brainina Kh., Neyman E.: *Electroanalytical Stripping Methods*. John Wiley and Sons, New York 1993.
2. Scholz F., Meyer B.: *Electroanalytical Chemistry, A Series of Advances* (A. J. Bard and I. Rubinstein, Eds), Vol. 20, p. 1. Marcel Dekker, New York 1998.
3. Jirkovský R.: *Mikrochemie* **1934**, 15, 331.
4. Engell H.-J.: *Z. Phys. Chem. (Leipzig)* **1956**, 7, 158.
5. Vermilyea D. A.: *J. Electrochem. Soc.* **1966**, 113, 1067.
6. Haruyama S., Masamura K.: *Corros. Sci.* **1978**, 18, 263.
7. Nicol M. J., Needs C. R. S.: *Electrochim. Acta* **1975**, 20, 585.
8. Nicol M. J., Needs C. R. S.: *Electrochim. Acta* **1977**, 22, 1381.
9. Vytřas K., Švancara I.: *Chem. Listy* **1994**, 88, 412.
10. Kuwana T., French W. G.: *Anal. Chem.* **1964**, 36, 241.
11. Ruby W. R., Tremmel C. G.: *J. Electroanal. Chem. Interfacial Electrochem.* **1968**, 18, 231.
12. Barikov V. G., Rozhdestvenskaya Z. B., Songina O. A.: *Zavod. Lab.* **1969**, 35, 776.
13. Brainina Kh. Z., Vydrevich M. B.: *J. Electroanal. Chem. Interfacial Electrochem.* **1981**, 121, 1.
14. Kalcher K., Kauffmann J.-M., Wang J., Švancara I., Vytřas K., Neuhold C., Yang Z.: *Electroanalysis (N. Y.)* **1995**, 7, 5.
15. Lecuire J.-M.: *J. Electroanal. Chem. Interfacial Electrochem.* **1975**, 66, 195.
16. Fitch A.: *Clays Clay Miner.* **1990**, 38, 391.
17. Walcarus A.: *Anal. Chim. Acta* **1999**, 384, 1.
18. Scholz F., Nitschke L., Henrion G.: *Naturwissenschaften* **1989**, 76, 71.
19. Scholz F., Nitschke L., Henrion G., Damaschun F.: *Naturwissenschaften* **1989**, 76, 167.
20. Rusling J. F., Suib S. L.: *Adv. Mater. (Weinheim, Ger.)* **1994**, 6, 922.
21. Scholz F., Meyer B.: *Chem. Soc. Rev.* **1994**, 23, 341.
22. Kulesza P. J., Cox J. A.: *Electroanalysis (N. Y.)* **1998**, 10, 73.
23. Moseley P. T., Norris J. O. W., Williams D. E.: *Techniques and Mechanisms in Gas Sensing*. Adam Hilger, New York 1991.
24. Kolb D.: *Angew. Chem.* **2001**, 113, 1198.
25. Mancey D. S., Shoesmith D. W., Lipkowski J., McBride A. C., Noël J.: *J. Electrochem. Soc.* **1993**, 140, 637.
26. White A. F., Peterson M. L., Hochella M. F.: *Geochim. Cosmochim. Acta* **1994**, 58, 1859.
27. Filmer A. O., MacLeod I. D., Parker A. J.: *Aust. J. Chem.* **1979**, 32, 975.
28. Yin Q., Vaughan D. J., England K. E. R., Kelsall G. H.: *J. Colloid Interface Sci.* **1994**, 166, 133.
29. Richardson P. E., O'Dell C. S.: *J. Electrochem. Soc.* **1985**, 132, 1350.
30. Wang X.-H., Ahlberg E., Forssberg K. S. E.: *Appl. Electrochem.* **1992**, 22, 1095.
31. Wei D., Osseo-Asare K.: *J. Electrochem. Soc.* **1996**, 143, 3192.
32. Franklin T. C., Nnodimelle R., Adeniyi W. K.: *J. Electrochem. Soc.* **1987**, 134, 2150.
33. Willig F.: *Adv. Electrochem. Electrochem. Eng.* **1981** 12, 1.
34. Eichhorn M., Willig F., Tesche B., Schulze W.: *Thin Solid Films* **1984**, 122, 287.
35. Bartlett P. N.: *J. Electroanal. Chem. Interfacial Electrochem.* **1991**, 300, 175.
36. Jansen R., Beck F.: *Electrochim. Acta* **1993**, 38, 907.
37. Švancara I., Vytřas K., Barek J., Zima J.: *Crit. Rev. Anal. Chem.* **2001**, 31, 311.
38. Gruner W., Kunath J., Kalnishevskaya L. N., Posokhin Yu. V., Brainina Kh. Z.: *Electroanalysis (N. Y.)* **1993**, 5, 243.

39. Rice M. E., Galus Z., Adams R. N.: *J. Electroanal. Chem. Interfacial Electrochem.* **1983**, 143, 89.

40. Zakharchuk N., Meyer S., Lange B., Scholz F.: *Croat. Chem. Acta* **2000**, 73, 667.

41. Moretti M. B., Zon A., Fernandez H., Rivas G., Solis V.: *Electrochem. Commun.* **1999**, 1, 472.

42. Eggins B. R., Hickey C., Toft S. A., Zhou D. M.: *Anal. Chim. Acta* **1997**, 347, 281.

43. Dahm R. H., Latham R. J., Mosley S. E.: *J. Appl. Electrochem.* **1986**, 16, 213.

44. Mouhandess M. T., Chassagneux F., Durand B., Sharara Z. Z., Vittori O.: *J. Mater. Sci.* **1985**, 20, 3289.

45. Encinas Bachiller P., Tascón García M. L., Vázquez Barbado M. D., Sánchez Batanero P.: *J. Electroanal. Chem.* **1997**, 424, 217.

46. Labrincha J. A., Meng L. J., Dos Santos M. P., Marques F. M. B., Frade J. R.: *Mater. Res. Bull.* **1993**, 28, 101.

47. Bauer D., Gaillochet M. Ph.: *Electrochim. Acta* **1974**, 19, 597.

48. Ramírez M. T., Palomar M. E., González I., Rojas-Hernández A.: *Electroanalysis* (N. Y.) **1995**, 7, 184.

49. Ghosh P. K., Bard A. J.: *J. Am. Chem. Soc.* **1983**, 105, 5691.

50. Liu H.-Y., Anson F. C.: *J. Electroanal. Chem. Interfacial Electrochem.* **1985**, 184, 411.

51. Shaw B. R., Creasy K. E., Lonczycki C. J., Sargeant J. A., Tirhado M.: *J. Electrochem. Soc.* **1988**, 135, 869.

52. Li Jian-wei, Calzaferri G.: *J. Chem. Soc., Chem. Commun.* **1993**, 1430.

53. Xiang Y., Villemure G.: *Clays Clay Miner.* **1996**, 44, 515.

54. Bard A. J.: *Integrated Chemical Systems*, p. 178. Wiley, New York 1994.

55. Bond A. M., Fletcher S., Marken F., Shaw S. J., Symons P. G.: *J. Chem. Soc., Faraday Trans.* **1996**, 92, 3925.

56. Doménech-Carbó A., Doménech-Carbó M. T., Gimeno-Adelantado J. V., Moya-Moreno M., Bosch-Reig F.: *Electroanalysis* (N. Y.) **2000**, 12, 120.

57. Doménech-Carbó A., Doménech-Carbó M. T., Moya-Moreno M., Gimeno-Adelantado J. V., Bosch-Reig F.: *Anal. Chim. Acta* **2000**, 407, 275.

58. Doménech-Carbó M. T., Casas-Catalán M. J., Doménech-Carbó A., Mateo-Castro R., Gimeno-Adelantado J. V., Bosch-Reig F.: *Fresenius' J. Anal. Chem.* **2001**, 369, 571.

59. Doménech-Carbó A., Doménech-Carbó M. T., Gimeno-Adelantado J. V., Bosch-Reig F., Saurí-Peris M. C., Casas-Catalán M. J.: *Fresenius' J. Anal. Chem.* **2001**, 369, 576.

60. Doménech-Carbó A., Doménech-Carbó M. T., Osete-Cortina L.: *Electroanalysis* (N. Y.) **2001**, 13, 927.

61. Roullier L., Laviron E.: *J. Electroanal. Chem. Interfacial Electrochem.* **1982**, 134, 181.

62. Blum D., Leyffer W., Holze R.: *Electronanalysis* (N. Y.) **1996**, 8, 296.

63. Manivannan A., Tryk D. A., Fujishima A.: *Chem. Lett.* **1999**, 851.

64. Waki S., Dokko K., Itoh T., Nishizawa M., Abe T., Uchida I.: *J. Solid State Electrochem.* **2000**, 4, 205.

65. da Silva Pereira M. I., da Costa F. M. A., Tavares A. C.: *Electrochim. Acta* **1994**, 11/12, 1571.

66. Hasse U., Scholz F.: *Electrochim. Commun.* **2001**, 3, 429.

67. Kanoh H., Feng Q., Miyai Y., Ooi K.: *J. Electrochem. Soc.* **1993**, 140, 3162.

68. Heller-Ling N., Prestat M., Gautier J.-L., Koenig J. F., Poillerat G., Chartier P.: *Electrochim. Acta* **1997**, 42, 197.

69. Tranchant A., Sarradin J., Messina R., Perichon J.: *Appl. Catal.* **1985**, 14, 289.

70. Lamache M., Bauer D.: *J. Electroanal. Chem. Interfacial Electrochem.* **1977**, *79*, 359.

71. Gavasso R., Laviron E.: *J. Electroanal. Chem. Interfacial Electrochem.* **1979**, *102*, 249.

72. Dostál A., Meyer B., Scholz F., Schröder U., Bond A. M., Marken F., Shaw Sh. J.: *J. Phys. Chem.* **1995**, *99*, 2096.

73. Zakharchuk N. F., Meyer B., Hennig H., Scholz F., Jaworski A., Stojek Z.: *J. Electroanal. Chem.* **1995**, *398*, 23.

74. Fiedler D. A., Besenhard J. O., Fooken M. H.: *J. Power Sources* **1997**, *69*, 157.

75. Fiedler D. A.: *J. Solid State Electrochem.* **1998**, *2*, 315.

76. Bezdička P., Grygar T., Klápník B., Vondrák J.: *Electrochim. Acta* **1999**, *45*, 913.

77. Bond A. M., Cooper J. B., Marken F., Way D. M.: *J. Electroanal. Chem.* **1995**, *396*, 407.

78. Wooster T. J., Bond A. M., Honeychurch M. J.: *Electrochim. Commun.* **2001**, *3*, 746.

79. Bond A. M., Miao W., Raston C. L.: *J. Phys. Chem. B* **2000**, *104*, 2320.

80. Bond A. M., Feldberg S. W., Miao W. J., Oldham K. B., Raston C. L.: *J. Electroanal. Chem.* **2001**, *501*, 22.

81. Fattakhova D., Kavan L., Krtík P.: *J. Solid State Electrochem.* **2001**, *5*, 196.

82. Schröder U., Scholz F.: *Inorg. Chem.* **2000**, *39*, 1006.

83. Shaw S. J., Marken F., Bond A. M.: *Electroanalysis (N. Y.)* **1996**, *8*, 732.

84. Shaw S. J., Marken F., Bond A. M.: *J. Electroanal. Chem.* **1996**, *404*, 227.

85. Meyer B., Ziemer B., Scholz F.: *J. Electroanal. Chem.* **1995**, *392*, 79.

86. Suarez M. F., Bond A. M., Compton R. G.: *J. Solid State Electrochem.* **1999**, *4*, 24.

87. Suarez M. F., Marken F., Compton R. G., Bond A. M., Miao W. J., Raston C. L.: *J. Phys. Chem. B* **1999**, *103*, 5637.

88. Schröder U., Meyer B., Scholz F.: *Fresenius' J. Anal. Chem.* **1996**, *356*, 295.

89. Bond A. M., Fletcher S., Symons P. G.: *Analyst (Amsterdam)* **1998**, *123*, 1891.

90. Schröder U., Scholz F.: *J. Solid State Electrochem.* **1997**, *1*, 62.

91. Bond A. M., Marken F., Hill E., Compton R. G., Hügel H.: *J. Chem. Soc., Perkin Trans. 2* **1997**, *1735*.

92. Fitch A., Du J., Gan H., Stucki J. W.: *Clays Clay Miner.* **1995**, *43*, 607.

93. Lange B., Scholz F., Weiss A., Schwedt G., Behnert J., Raezke K.-P.: *Int. Lab.* **1993**, *23*, 23.

94. Mouhandess M. T., Chassagneux F., Vittori O., Accary A., Reeves R. M.: *J. Electroanal. Chem. Interfacial Electrochem.* **1984**, *181*, 93.

95. Grygar T.: *J. Solid State Electrochem.* **1998**, *2*, 127.

96. Clauss C. R. A., Schweigert H. E. L. G.: *J. Electrochem. Soc.* **1976**, *123*, 951.

97. Chabre Y. P.: *J. Electrochem. Soc.* **1991**, *138*, 329.

98. Gervasi C. A., Biaggio S. R., Vilche J. R., Arvia A. J.: *Electrochim. Acta* **1991**, *36*, 2147.

99. Gervasi C. A., Vilche J. R., Alvarez P. E.: *Electrochim. Acta* **1996**, *41*, 455.

100. Grygar T.: *Collect. Czech. Chem. Commun.* **1996**, *61*, 93.

101. Maskell W. C.: *J. Electroanal. Chem. Interfacial Electrochem.* **1986**, *199*, 127.

102. Lovrić M., Hermes M., Scholz F.: *J. Solid State Electrochem.* **2000**, *4*, 394.

103. Scholz F., Lange B., Jaworski A., Pelzer J.: *Fresenius' J. Anal. Chem.* **1991**, *340*, 140.

104. Grygar T., Šubrt J., Boháček J.: *Collect. Czech. Chem. Commun.* **1995**, *60*, 950.

105. Doménech-Carbó A., Sánchez-Ramos S., Doménech-Carbó M. T., Gimeno-Adelantado J. V., Bosch-Reig F., Yusá-Marco D. J., Saurí-Peris M. C.: *Electroanalysis (N. Y.)*, in press.

106. Brainina Kh. Z., Lesunova R. P.: *Zh. Anal. Khim.* **1974**, *29*, 1302.

107. Grygar T., van Oorschot I. H. M.: *Electroanalysis (N. Y.)*, in press.

108. Grygar T.: *J. Electroanal. Chem.* **1996**, *405*, 117.

109. Doménech-Carbó A., Doménech-Carbó M. T., Gimeno-Adelantado J. V., Bosch-Reig F., Saurí-Peris M. C., Sánchez-Ramos S.: *Analyst (Amsterdam)* **2001**, 126, 1764.

110. Grygar T., Bezdička P.: *J. Solid State Electrochem.* **1998**, 3, 31.

111. Bakardjieva S., Bezdička P., Grygar T., Vorm, P.: *J. Solid State Electrochem.* **2000**, 4, 306.

112. Grygar T.: *J. Solid State Electrochem.* **1997**, 1, 77.

113. Lamache M., Bauer D.: *Anal. Chem.* **1979**, 51, 1320.

114. Brage M. C., Lamache M., Bauer D.: *Electrochim. Acta* **1979**, 24, 25.

115. Scholz F., Lange B.: *Fresenius' J. Anal. Chem.* **1990**, 338, 293.

116. Komorsky-Lovrić Š., Bartoll J., Stösser R., Scholz F.: *Croat. Chem. Acta* **1997**, 70, 563.

117. Grygar T., Dědeček J., Hradil D.: *Geol. Carpathica*, submitted.

118. Zejnilović R. M., Blagojević N., Jović V. D., Despić A. R.: *Anal. Chim. Acta* **1996**, 327, 107.

119. Cepriá G., Abadias O., Pérez-Arantegui J., Castillo J. R.: *Electroanalysis (N. Y.)* **2001**, 13, 477.

120. Scholz F., Müller W.-D., Nitschke L., Rabi F., Livanova L., Fleischfresser C., Thierfelder Ch.: *Fresenius' J. Anal. Chem.* **1990**, 338, 37.

121. Scholz F., Rabi F., Müller W.-D.: *Electroanalysis (N. Y.)* **1992**, 4, 339.

122. Lux L., Gálová M., Heželová M., Markušová K.: *J. Solid State Electrochem.* **1999**, 3, 288.

123. Gálová M., Oriňáková R., Grygar T., Lux L., Heželová M.: *Part. Sci. Technol.* **2001**, 19, 85.

124. Scholz F., Nitschke L., Henrion G.: *Electroanalysis (N. Y.)* **1990**, 2, 85.

125. Doménech-Carbó A., Doménech-Carbó M. T., Osete-Cortina L., Gimeno-Adelantado J. V., Bosch-Reig F., Mateo-Castro R.: *Talanta* **2002**, 56, 161.

126. Carbonnelle P., Lamberts L.: *Electrochim. Acta* **1992**, 37, 1321.

127. Meyer B., Zhang S., Scholz F.: *Fresenius' J. Anal. Chem.* **1996**, 356, 267.

128. Bond A. M., Scholz F.: *J. Geochem. Explor.* **1992**, 42, 227.

129. Zhang S., Meyer B., Moh G., Scholz F.: *Electroanalysis (N. Y.)* **1995**, 7, 319.

130. Brainina Kh. Z., Lesunova R. P., Serebryakova L. N.: *Zavod. Lab.* **1974**, 40, 632

131. Bennouna A., Durand B., Vittori O.: *Electrochim. Acta* **1987**, 32, 713.

132. Bennouna A., Durand B., Vittori O.: *Electrochim. Acta* **1987**, 32, 1337.

133. Bennouna A., Durand B., Vittori O.: *Electrochim. Acta* **1991**, 36, 1505.

134. Scholz F., Nitschke L., Kemnitz E., Olesch T., Henrion G., Hass D., Bagchi R. N., Herrmann R., Pruss N., Wilde W.: *Fresenius' J. Anal. Chem.* **1989**, 335, 571.

135. Scheurell S., Scholz F., Olesch T., Kemnitz E.: *Supercond. Sci. Technol.* **1992**, 5, 303.

136. Mouhandess M. T., Chassagneux F., Vittori O.: *J. Electroanal. Chem. Interfacial Electrochem.* **1982**, 131, 367.

137. Sharara Z. Z., Vittori O., Durand B.: *Electrochim. Acta* **1984**, 29, 1685.

138. Sharara Z. Z., Vittori O., Durand B.: *Electrochim. Acta* **1984**, 29, 1689.

139. De Guzman R. N., Shen Y. F., Shaw B. R., Suib S. L., Young C. L.: *Chem. Mater.* **1993**, 5, 1395.

140. Komorsky-Lovrić Š.: *Croat. Chem. Acta* **1998**, 71, 263.

141. Centeno B., Tascón M. L., Vázquez M. D., Sánchez Batanero P.: *Electrochim. Acta* **1991**, 36, 277.

142. Adekola F. A., Colin C., Bauer D.: *Electrochim. Acta* **1992**, 37, 2009.

143. de Castro-Martins S., Khouzami S., Tuel A., Ben Taarit Y., El Murr N., Sellami A.: *J. Electroanal. Chem.* **1993**, 350, 15.

144. de Castro-Martins S., Tuel A., Ben Taarit Y.: *Zeolites* **1994**, 14, 130.

145. Doménech A., Corma A., García H., Valencia S.: *Top. Catal.* **2000**, *11*, 401.

146. Bodoardo S., Geobaldo F., Penazzi N., Arrabito M., Rivetti F., Spano G., Lamberti C., Zecchina A.: *Electrochem. Commun.* **2000**, *2*, 349.

147. Eguren M., Tascón M. L., Vázquez M. D., Sánchez Batanero P.: *Electrochim. Acta* **1988**, *33*, 1009.

148. Haber J., Nowak P.: *Catal. Lett.* **1994**, *27*, 369.

149. McBreen J.: *Electrochim. Acta* **1975**, *20*, 221.

150. Kleber W.: *Einführung in die Kristallographie*, p. 191. VEB Verlag der Technik, Berlin 1974.

151. Bond A. M., Scholz F.: *Langmuir* **1991**, *7*, 3197.

152. Reddy S. J., Dostál A., Scholz F.: *J. Electroanal. Chem.* **1996**, *403*, 209.

153. Schwudke D., Stösser R., Scholz F.: *Electrochem. Commun.* **2000**, *2*, 301.

154. Grygar T., Bakardjieva S., Bezdička P., Vorm P.: *Ceramics–Silikáty* **2001**, *45*, 55.

155. Grygar T., Bezdička P., Piszora P., Wolska E.: *J. Solid State Electrochem.* **2001**, *5*, 487.

156. Grygar T., Bezdička P., Vorm P., Jordanova N., Krtík P.: *J. Solid State Chem.* **2001**, *161*, 152.

157. Sigala C., Verbaere A., Mansot J. L., Guyomard D., Piffard Y., Tournoux M.: *J. Solid State Chem.* **1997**, *132*, 372.

158. Obrovac M. N., Gao Y., Dahn J. R.: *Phys. Rev. B: Condens. Matter* **1998**, *57*, 5728.

159. Ohzuku T., Takeda S., Iwanaga M.: *J. Power Sources* **1999**, *82*, 90.

160. Kawai H., Nagata M., Tabuchi M., Tukamoto H.: West A. R.: *Chem. Mater.* **1998**, *10*, 3266.

161. Kawai H., Nagata M., Kageyama H., Tukamoto H., West A. R.: *Electrochim. Acta* **1999**, *45*, 315.

162. Ohzuku T., Ariyoshi K., Takeda S., Sakai Y.: *Electrochim. Acta* **2001**, *46*, 2327.

163. Liu W., Kowal K., Farrington G. C.: *J. Electrochem. Soc.* **1998**, *145*, 459.

164. Mukerjee S., Thurston T. R., Jisrawi N. M., Yang X. Q., McBreen J., Daroux M. L., Xing X. K.: *J. Electrochem. Soc.* **1998**, *145*, 466.

165. Ohzuku T., Ueda A., Nagayama M.: *J. Electrochem. Soc.* **1993**, *140*, 1862.

166. Delmas C., Ménétrier M., Croguennec L., Saadoune I., Rougier A., Pouillerie C., Prado G., Grüne M., Fournès L.: *Electrochim. Acta* **1999**, *45*, 243.

167. Grygar T., Bezdička P., Caspary E.-G.: *J. Electrochem. Soc.* **1999**, *146*, 3234.

168. Tarascon J. M., Guyomard D.: *J. Electrochem. Soc.* **1991**, *138*, 2864.

169. Sapozhnikova E. Ya., Davidovich A. G., Roizenblat E. M., Zinovik M. A., Kosheleva L. V., Maslova V. M., Markovskii E. V.: *Zh. Neorg. Khim.* **1981**, *26*, 1751.

170. Sapozhnikova E. Ya., Davidovich A. G., Roizenblat E. M., Zinovik M. A., Markovskii E. V., Kosheleva L. V.: *Zh. Neorg. Khim.* **1982**, *27*, 2888.

171. Dostál A., Schröder U., Scholz F.: *Inorg. Chem.* **1995**, *34*, 1711.

172. Scholz F., Dostál A.: *Angew. Chem., Int. Ed. Engl.* **1996**, *34*, 2685.

173. Barcena-Soto M., Scholz F.: *J. Electroanal. Chem.*, in press.

174. Pereira-Ramos J.-P., Messina R., Perichon J.: *J. Electroanal. Chem. Interfacial Electrochem.* **1983**, *146*, 157.

175. Baker M. D., Zhang J.: *J. Phys. Chem.* **1990**, *94*, 8703.

176. Li Jian-wei, Calzaferri G.: *J. Electroanal. Chem.* **1994**, *377*, 163.

177. El Murr N., Kerkeni M., Sellami E., Ben Taarit Y.: *J. Electroanal. Chem. Interfacial Electrochem.* **1988**, *246*, 461.

178. Venkatathri N., Vinod M. P., Vijaymohan K., Sivasanker S.: *J. Chem. Soc., Faraday Trans.* **1996**, 92, 473.

179. Bedioui F., Briot E., Devynck J., Balkus K. J.: *Inorg. Chim. Acta* **1997**, 254, 151.

180. Beck F., Barsch U.: *J. Electroanal. Chem. Interfacial Electrochem.* **1990**, 282, 175.

181. Barsch U., Beck F.: *Electrochim. Acta* **1990**, 35, 759.

182. Burnham A. K., Braun R. L.: *Energy Fuels* **1999**, 13, 1.

183. Boudreau B. P., Ruddick B. R.: *Am. J. Sci.* **1991**, 291, 507.

184. Postma D.: *Geochim. Cosmochim. Acta* **1993**, 57, 5027.

185. Schmalzried H.: *Chemical Kinetics of Solids*. VCH, Weinheim 1995.

186. Gielen M., Willem R., Wrackmeyer B.: *Solid State Organometallic Chemistry: Methods and Applications*. Wiley, New York 1999.

187. Ohashi Y.: *Reactivity in Molecular Crystals*. VCH, Weinheim 1993.

188. Chlistunoff J., Cliffel D., Bard A. J.: *Thin Solid Films* **1995**, 257, 166.

189. Komorsky-Lovrić S., Lovrić M., Scholz F.: *Mikrochim. Acta* **1997**, 127, 95.

190. Bond A. M., Colton R., Marken F., Walter J. N.: *Organometallics* **1994**, 13, 5122.

191. Bond A. M., Marken F.: *J. Electroanal. Chem.* **1994**, 372, 125.

192. Reddy S. J., Hermes M., Scholz F.: *Electroanalysis (N. Y.)* **1996**, 8, 955.

193. Eklund J. C., Bond A. M.: *J. Am. Chem. Soc.* **1999**, 121, 8306.

194. Pletcher D., Walsh F. C.: *Industrial Electrochemistry*. Blackie Academic & Professional, London 1993.

195. Bond A. M., Marken F., Williams C. T., Beattie D. A., Keyes T. E., Forster R. J., Vos J. G.: *J. Phys. Chem. B* **2000**, 104, 1977.

196. Bond A. M., Scholz F.: *J. Phys. Chem.* **1991**, 95, 7460.